Published May 11, 2009

hearing loss (5). The urticarial rash observed in CAPS is similar to that associated with common urticaria. However, unlike the latter disorder, the rash observed in most CAPS patients responds to therapy with IL-1 receptor antagonist rather than antihistamines, suggesting that urticaria in these patients is mediated by IL-1. However, the cellular mechanism responsible for urticaria in CAPS patients remains poorly understood.

The mature form of IL-1β is produced by cleavage of the inactive pro–IL-1β precursor by caspase-1, a protease activated by a large multiprotein complex termed the inflammasome (6). CAPS is caused by missense mutations in the gene, nucleotide-binding oligomerization domain (NOD)–leucine-rich repeats (LRRs) containing pyrin domain 3 (*NLRP3*) (7), whose product is a component of the inflammasome that includes the adaptor protein, apoptosis-associated speck-like protein containing a caspase recruitment domain (ASC), and procaspase-1 (8, 9). NLRP3, a member of the NOD-like receptor family, is an intracellular receptor involved in the recognition of pathogen-associated molecular patterns (PAMPs). Although several microbial activators of NLRP3 have been reported, the precise mechanism by which the NLRP3 inflammasome is activated by PAMPs remains poorly understood. In the presence of ATP or pore-forming molecules, several PAMPs, including LPS, muramyl dipeptide, bacterial mRNA, and the antiviral compound R837, activate the NLRP3 inflammasome (10, 11). In addition to PAMPs, NLRP3 senses endogenous danger signals such as monosodium urate crystals and particulate matter including asbestos, silica (12), and aluminum salts (13, 14). Disease-associated NLRP3 mutations associated with CAPS localize to the centrally located NOD domain and constitutively activate caspase-1 to produce active IL-1β (8, 15). NLRP3 is predominantly expressed in monocytes, granulocytes, and chondrocytes (16, 17), but to date, no reports have investigated the cells in the skin that are involved in the development of urticarial rash associated with CAPS. Our study identifies resident MCs in the skin as a cell population capable of producing IL-1β via the NLRP3 inflammasome and provides evidence that MCs mediate urticarial rash via dysregulated IL-1β production in the skin of CAPS patients.

RESULTS

Resident MCs produce constitutively mature IL-1β in CAPS skin

To identify the source of IL-1β in the human skin, we performed immunolabeling of skin organ cultures with an antibody (Ab) that recognizes p17, the mature form of IL-1β. Expression of mature IL-1β was undetectable in normal skin cells but was induced in resident cells by incubation of skin organ cultures with LPS and R837 (Fig. 1). In contrast, cells in the dermis of two MWS patients harboring the E567K or K355T *NLRP3* mutation and suffering from active disease but not receiving any treatment expressed the mature form of IL-1β constitutively without any stimulation (Fig. 1). Notably, the majority of the mature IL-1β–positive cells colocalized with avidin-FITC (Fig. 1), which specifically labels tryptase-positive MCs, but not with HLA-DR, -DP, -DQ, a marker of DCs and macrophages (Fig. S1), in both normal and CAPS skin.

MCs express inflammasome components and produce IL-1β in response to proinflammatory stimuli

We next analyzed the expression of inflammasome components in MCs using mouse bone marrow–derived cultured MCs (BMCMCs). The purity of cultured MCs, which was >97%, was confirmed by surface expression of CD45 and Kit, as well as FITC-avidin labeling. Exclusion of DCs/macrophages was further supported by the lack of $I\text{-}A^b$ expression in the MC population (Fig. S2 A). BMCMCs constitutively expressed *Casp1* and the critical adaptor *Asc*, as determined

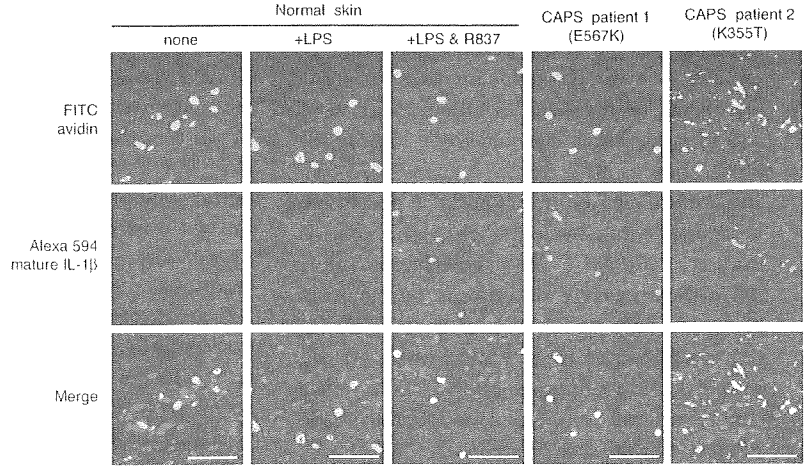

Figure 1. MCs from the skin of CAPS patients expressing disease-associated NLRP3 mutations constitutively express the mature form of IL-1β. Human skin specimens were stained with FITC-avidin to label MCs (top) and Alexa Fluor 594–conjugated anti–IL-1β Ab that recognizes only the mature form of IL-1β (middle). (bottom) Overlay of fluorescence images of the top and middle panels. The nuclei were counterstained with Hoechst 33342 (blue). Normal skin represents organ skin cultures with or without incubation with 100 ng/ml LPS or LPS and 100 µM R837 for 24 h. Results are representative of at least three separate experiments. Bars, 50 µm.

Published May 11, 2009

by RT-PCR analysis (Fig. 2, A and B). In contrast, there was no or little expression of *Nlrp3* and *Il1b* in MCs, but both genes were induced by stimulation with LPS (Fig. 2, A and B), which is consistent with what was reported in human monocytes (18). Induction of *Nlrp3* and *Il1b* by LPS was reduced by treatment with MG-132, a broad proteasome inhibitor that can affect several signaling pathways including NF-κB (Fig. 2 A), suggesting that induction of *Nlrp3* and *Il1b* may require NF-κB activation.

We next determined the ability of MCs to produce IL-1β in response to proinflammatory stimuli known to activate caspase-1. Stimulation of MCs with LPS alone induced little IL-1β secretion, whereas treatment with R837, a small antiviral synthetic compound that activates the NLRP3 inflammasome (11), induced potent IL-1β secretion in MCs pretreated with LPS (Fig. 2, C and D). In accordance with these results, R837 effectively induced intracellular processing of pro–IL-1β into p17 in LPS-primed MCs, whereas secretion of mature IL-1β into the culture supernatant was more potently induced by ATP than by R837 (Fig. 2 D). BMCMCs did not express *Tlr7* mRNA as assessed by real-time PCR (not depicted) and Tlr7 protein by immunoblotting (Fig. S2 B), suggesting that R837 promotes caspase-1 activation independently of Tlr7 in MCs. In contrast, incubation of MCs with LPS alone was sufficient to induce secretion of TNF-α and IL-6 (Fig. 2, E and F). Notably, co-stimulation with LPS and R837 did not induce MC degranulation as determined by the release of β-hexosaminidase (Fig. 2 G) and histamine (Fig. 3 A, right), indicating that the mechanisms involved in IL-1β secretion and degranulation are differentially regulated in MCs.

ATP stimulation through the purinergic P2X, ligand-gated ion channel 7 receptor (P2X7R) is essential for the activation of the NLRP3 inflammasome in macrophages (10, 19). We found that in addition to R837, ATP induced secretion of IL-1β in MCs stimulated with LPS (Fig. 2 D; and Fig. 3 A, left), which is consistent with the expression of the P2x7r in MCs (20). K^+ efflux induced by ATP is important for caspase-1 activation via P2x7r (21), and this ion channel rapidly transitions to a pore-like structure that allows passage of molecules as large as 900 D (19). Notably, IL-1β secretion induced by ATP or R837 was completely abrogated when the MCs were incubated in medium containing a high K^+ concentration (Fig. 3 B). Furthermore,

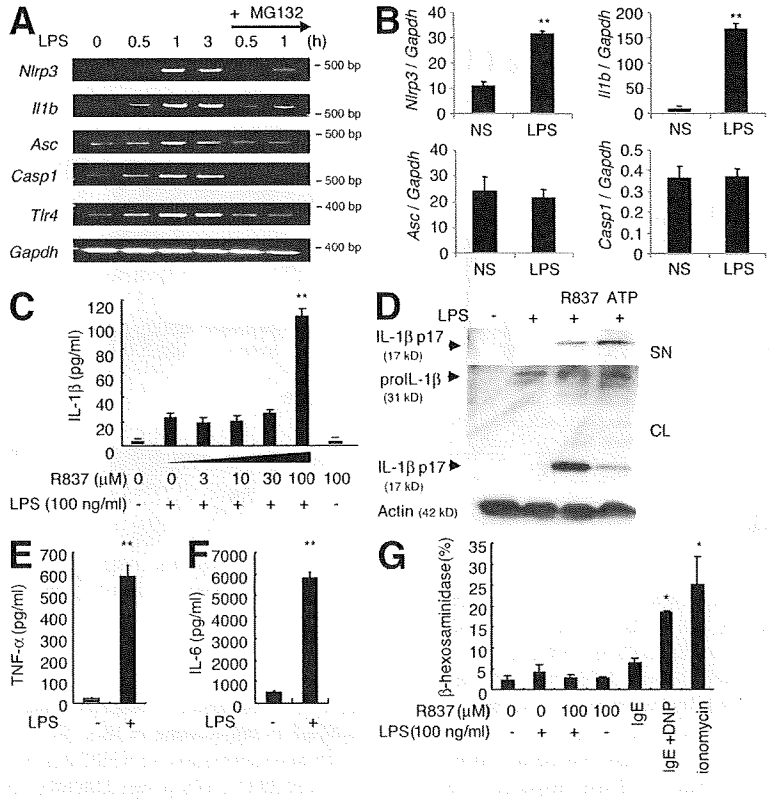

Figure 2. Activation of inflammasome with LPS and R837 induces IL-1β secretion but not degranulation in MCs. (A) Semiquantitative RT-PCR analysis of *Nlrp3*, *Il1b*, *Asc*, *Casp1*, and *Tlr4* in mouse BMCMCs stimulated with 100 ng/ml LPS. 5 μM MG132 was added 30 min before LPS stimulation. (B) Expression of specific mRNAs after stimulation for 3 h with 100 ng/ml LPS in BMCMCs was quantified by real-time PCR and normalized to *Gapdh* expression (×10^4). (C) BMCMCs were pretreated with LPS for 15 h and stimulated by R837 for 30 min. IL-1β levels in supernatants were measured by ELISA. (D) Immunoblot analysis of cultured supernatant (SN) and cell lysate (CL) from BMCMCs incubated with the indicated stimuli. (E and F) BMCMCs were stimulated with 100 ng/ml LPS for 15 h, and the amounts of TNF-α and IL-6 in culture supernatants were measured by ELISA. (G) Degranulation of BMCMCs was assessed by the release of β-hexosaminidase. Error bars represent means ± SD of triplicates. All results are representative of at least three separate experiments. *, $P < 0.005$; and **, $P < 0.001$ compared with untreated BMCMCs. NS, not stimulated.

Published May 11, 2009

ATP induced large pore formation in MCs as determined by YoPro-1 staining (Fig. 3 C, left), which was not observed in P2x7r-deficient MCs (Fig. 3 C, right). Unlike ATP, R837 did not induce large pore formation (Fig. 3 C, left) even though R837 is structurally related to ATP. However, secretion of IL-1β induced by ATP required expression of P2x7r in LPS-stimulated MCs as well as that elicited by R837 was also dependent, at least in part, on P2x7r (Fig. 3 D). These results suggest that the P2x7r and K^+ efflux are important for both ATP- and R837-induced secretion of IL-1β in MCs.

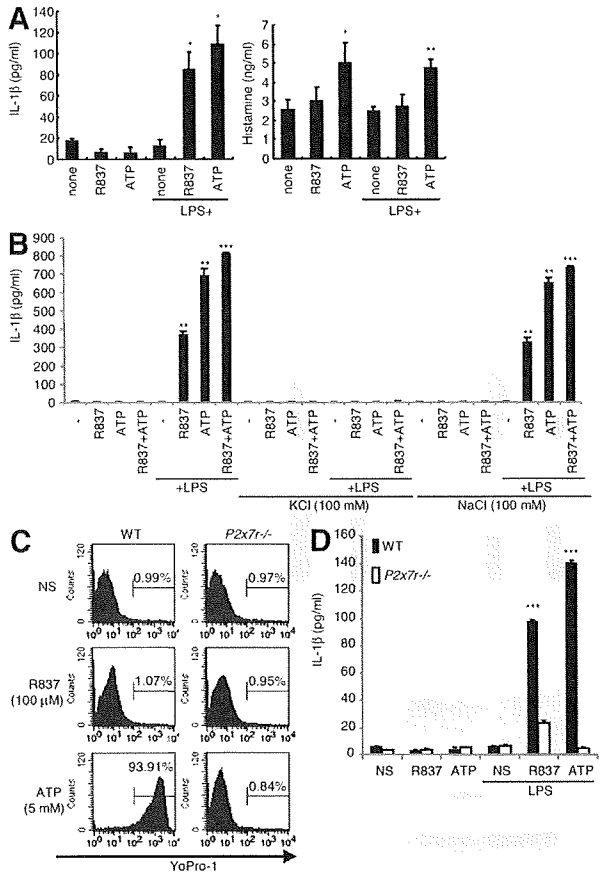

Figure 3. IL-1β secretion induced by R837 and ATP is mediated via P2x7r and K^+ efflux in MCs. (A, left) IL-1β secretion from BMCMCs. BMCMCs were cultured with or without LPS for 15 h and then stimulated with 5 mM ATP or 100 μM R837. (right) Histamine release from BMCMCs was analyzed by ELISA (same samples as in the left panel). (B) BMCMCs were cultured with or without LPS for 15 h. Medium containing 100 mM KCl or 100 mM NaCl was added for the last 30 min of culture at the same time as ATP or R837. IL-1β was measured in cell-free supernatants. (C) 2 mM YoPro-1 was added 10 min before BMCMCs were left untreated (NS) or stimulated with 5 mM ATP or 100 μM R837 for 30 min, and fluorescence intensity was analyzed by FACS. (D) BMCMCs were incubated with the indicated stimuli, and IL-1β was measured in cell-free supernatants. Error bars represent means ± SD of triplicates. All results are representative of at least three separate experiments. *, $P < 0.005$; **, $P < 0.001$; and ***, $P < 0.0001$ compared with untreated BMCMCs or between WT and mutant MCs. NS, not stimulated.

IL-1β secretion from MCs depends on the Nlrp3 inflammasome

To determine if the inflammasome is required for IL-1β secretion in MCs, we prepared MCs from WT and mutant mice deficient in Nlrp3, Nlrc4, or Asc. Stimulation of WT and mutant MCs lacking Nlrc4, a NOD-like receptor family member involved in inflammasome activation in response to flagellin (22, 23), induced processing of procaspase-1 into the mature p20 fragment (Fig. 4 A, top). In contrast, production of the processed p20 caspase-1 subunit was impaired in MCs deficient in Nlrp3 or Asc (Fig. 4 A, middle and bottom). Consistently, IL-1β secretion was not detected in MCs from Nlrp3- or Asc-deficient mice in response to LPS plus ATP or R837 (Fig. 4 B, top), whereas that produced by MCs lacking Nlrc4 was unimpaired when compared with WT MCs (Fig. S3, top). The lack of IL-1β secretion in MCs deficient in Nlrp3 or Asc was specific in that production of TNF-α and IL-6 was maintained in WT and mutant MCs (Fig. 4 B, middle and bottom; and Fig. S3, middle and bottom), although the amounts of both cytokines was reduced in MCs lacking Nlrp3 (Fig. 4 B, middle and bottom).

We next assessed the expression of inflammasome components in other populations of MCs. In mice, MCs are often divided into connective tissue– and mucosal-type MCs. Mouse fetus skin–derived MCs (FSMCs) are often used as a model of connective tissue–type MCs (24) that are distributed

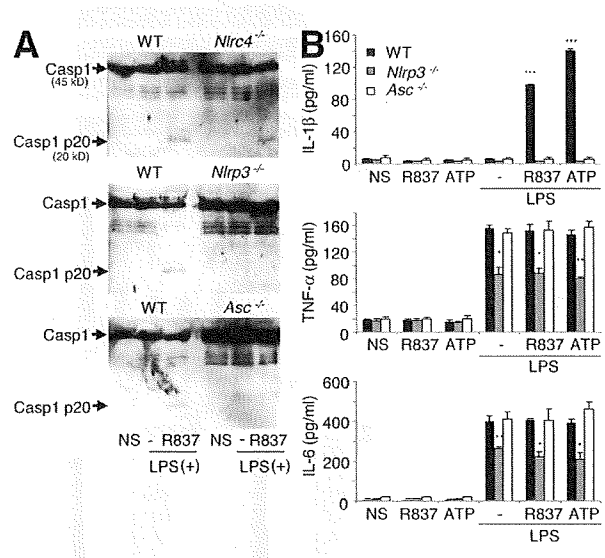

Figure 4. Activation of caspase-1 and IL-1β secretion requires the Nlrp3 inflammasome in MCs. (A) Immunoblot analysis of total cell extracts and supernatant from BMCMCs. Processing of procaspase-1 induced by R837 in LPS-primed BMCMCs from WT, Nlrc4-deficient (*Nlrc4*$^{-/-}$), Nlrp3-deficient (*Nlrp3*$^{-/-}$), and Asc-deficient (*Asc*$^{-/-}$) mice. Cells were pretreated with 100 ng/ml LPS and then stimulated with 100 μM R837. Casp1, procaspase-1; Casp1 p20, cleaved product of caspase-1. (B) Secretion of IL-1β, TNF-α, and IL-6 by LPS-stimulated BMCMCs from the indicated mice in response to R837 or ATP. Error bars represent means ± SD of triplicates. All results are representative of at least three separate experiments. *, $P < 0.005$; **, $P < 0.001$; and ***, $P < 0.0001$ compared between WT and mutant MCs. NS, not stimulated.

Published May 11, 2009

in the dermis. We found that the expression of *Nlrp3*, *Asc*, and *Il1b* was low in unstimulated FSMCs but enhanced after LPS treatment, as it was shown in BMCMCs (Fig. S4 A). Similarly, the pattern of IL-1β secretion and MC degranulation was comparable in BMCMCs and FSMCs (Fig. S4, B and C). Likewise, human MCs derived from cord blood progenitors cultured with stem cell factor expressed *ASC*, *NLRP3*, and *IL1B* after LPS stimulation (Fig. S5 A). Similar to that reported in human monocytes (25), incubation of human MCs with LPS alone was sufficient to induce the processing of pro–IL-1β into the mature form of IL-1β (p17), which was enhanced by R837 or ATP (Fig. S5, B and C).

Constitutive activation of the inflammasome by disease-associated Nlrp3 mutants in MCs

CAPS-associated NLRP3 mutations exhibit constitutive ASC-dependent NF-κB activation when expressed in tumor cell lines (17, 26). To assess the function of mutant NLRP3, we generated mouse Nlrp3 mutants (R258W, D301N, and Y570C) corresponding to the major CAPS-associated mutations (R260W, D303N, and Y570C, respectively) and tested their ability to induce NF-κB activation by luciferase reporter assay. In agreement with human studies, all three Nlrp3 mouse mutants as well as the Nlrp3 mutant lacking the LRR exhibited constitutive Asc-dependent NF-κB activation in HEK293 cells (Fig. 5 A). To further assess the function of disease-associated mutants, we introduced WT and mutant Nlrp3 into BMCMCs using a retroviral expression system that simultaneously coexpresses GFP. After normalization for the number of GFP-expressing cells, we found that the secretion of IL-1β was significantly higher in MCs producing disease-associated Nlrp3 mutants than in cells expressing WT protein after stimulation with LPS (Fig. 5 B). Notably, the increased production of IL-1β induced by Nlrp3 mutants R258W and Y570C was abolished when their pyrin domain was deleted (ΔPYD_R258W and ΔPYD_Y570C; Fig. 5 B), which is consistent with a critical role for the pyrin domain in the interaction with caspase-1 through the adaptor Asc.

To further study the function of disease-associated Nlrp3 mutant in MCs, we stably expressed WT and the common R258W mutant in the MC line MC/9 by retroviral infection (Fig. S6). MC/9 cells constitutively expressed *Nlrp3*, *Asc*, *Casp1*, and *Tlr4* but little or no *Il1b* in the absence of LPS (Fig. 5 C). Expression of *Il1b* was induced by LPS (Fig. 5 C). Importantly, unlike MC/9 cells expressing the CAPS-associated R258W mutant, cells transduced with control GFP vector or producing WT-Nlrp3 required stimulation with both LPS and ATP or R837, two stimuli that activate the Nlrp3

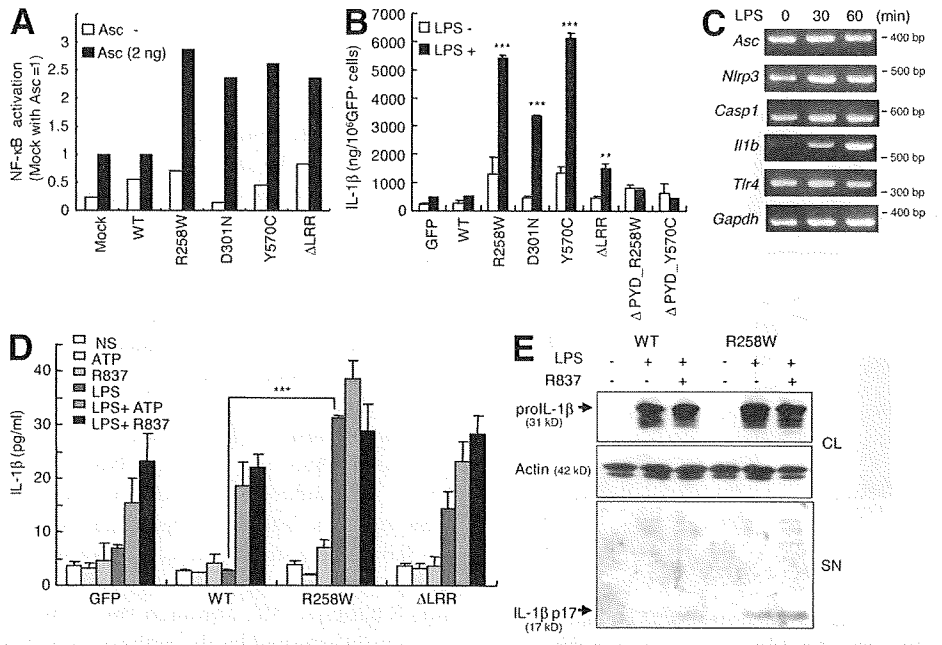

Figure 5. Expression of disease-associated Nlrp3 mutants induce constitutive activation of the inflammasome in MCs. (A) Constructs expressing WT, mutants (R258W, D301N, and Y570C), or Nlrp3 lacking LRR (ΔLRR) were transfected in the presence and absence of Asc plasmid into HEK293 cells. NF-κB activation was assessed by a dual luciferase reporter assay. Values represent the fold increase over that observed by transfection with control or Asc plasmid alone, which was considered as 1. (B) BMCMCs expressing GFP, WT, mutants, and mutants lacking the pyrin (ΔPYD_R258W and ΔPYD_Y570C) by retroviral infection were stimulated with LPS or left untreated. IL-1β was measured by ELISA and normalized to the number of GFP⁺ cells, as previously described (reference 47). **, $P < 0.001$; and ***, $P < 0.0001$ versus LPS-stimulated BMCMCs transfected with WT plasmid. (C) RT-PCR for gene expression in MC/9 cells stimulated with LPS. (D) MC/9 cells stably expressing GFP, WT, mutant Nlrp3, or ΔLRR were stimulated with LPS for 15 h, and then stimulated with ATP or R837. IL-1β secretions were measured by ELISA. ***, $P < 0.0001$ versus LPS-stimulated MC/9 cells expressing WT plasmid. Error bars in B and D represent means ± SD of triplicates. (E) Immunoblot analysis of culture supernatant (SN) and cell lysate (CL) from MC/9 cells stably expressing WT or R258W, and incubated with the indicated stimuli. All results are representative of at least three separate experiments.

Published May 11, 2009

inflammasome, for IL-1β secretion (Fig. 5 D). Although stimulation with LPS alone induced the production of pro–IL-1β in MC/9 cells expressing either WT or mutant Nlrp3, the processed p17 form of mature IL-1β could be detected only in the culture supernatant of MC/9 cells expressing the R258W mutant (Fig. 5 E). In contrast and consistent with results presented in Figs. 2–4, the secretion of mature IL-1β in MC/9 cells expressing WT-Nlrp3 required stimulation with both LPS and R837, which was enhanced in cells producing the CAPS-associated Nlrp3 mutant (Fig. 5 E).

To assess the effect of disease-associated Nlrp3 in vivo, we injected MC/9 cells expressing either WT or mutant Nlrp3 i.p. into mice and assessed the recruitment of neutrophils in the i.p. cavity. FACS analysis revealed that MC/9 cells expressing mutant R258W but not WT-Nlrp3 constitutively produced intracellular IL-1β after injection into the peritoneal cavity (Fig. 6 A). At 36 h after injection, the number of Gr-1$^+$ neutrophils was significantly increased in the peritoneal cavity of mice injected with MC/9 cells expressing mutant R258W-Nlrp3 compared with that found in mice injected with cells expressing WT-Nlrp3 (Fig. 6 B). In contrast, administration of ionomycin, but not MCs expressing WT or mutant Nlrp3, increased the levels of histamine in the peritoneal cavity (Fig. 6 C). Collectively, these results indicate that disease-associated Nlrp3 mutants induce constitutive production of IL-1β but not histamine release, and promote neutrophil recruitment when expressed in MCs.

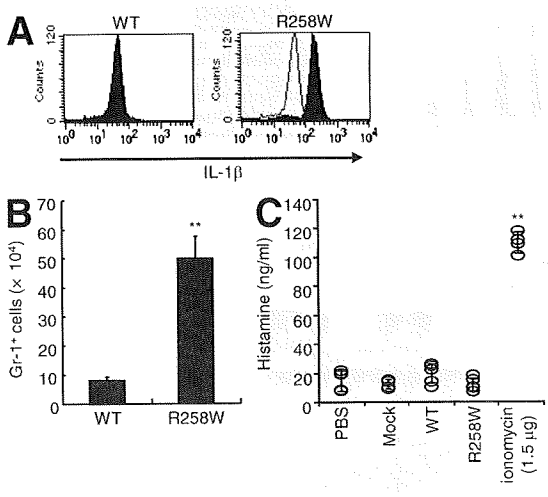

Figure 6. MCs expressing disease-associated Nlrp3 mutant promote neutrophil recruitment but not histamine release in the mouse peritoneal cavity. MC/9 cells stably expressing WT or R258W-Nlrp3 were injected into the mouse peritoneal cavity. Results were obtained 36 h after injection. (A) Shaded histograms represent intracellular IL-1β expression in MC/9 cells. The open histogram corresponds to labeling with isotype-matched control Ab. (B) Gr-1$^+$ cells in the peritoneal fluid. (C) The amounts of histamine in the peritoneal cavity 36 h after the injection of MC/9 cells. As a positive control, 1.5 μg ionomycin was injected 15 min before sample collection. Error bars represent means ± SD of triplicates. All results are representative of at least three separate experiments. **, $P < 0.001$ ($n = 5$ mice per group).

Induction of neutrophil-rich inflammation and vascular leakage by MCs expressing disease-associated Nlrp3 mutant

Urticarial rash in CAPS skin is characterized histologically by the presence of neutrophils and edema in the dermis (27). To study the role of IL-1β produced by MCs in vivo, we injected MC/9 cells expressing WT or mutant Nlrp3 (R258W) into the mouse skin. Histopathological analysis revealed the presence of neutrophils and edema in the dermis of the mouse ear at the site of injection, with MC/9 cells expressing R258W-Nlrp3 in a pattern that was similar to that observed in the involved skin of human CAPS (Fig. 7 A). In contrast, injection with MC/9 cells expressing WT-Nlrp3 induced minimal or no neutrophilic infiltrate or edema in the dermis of the mouse ear (Fig. 7 A). Furthermore, there was enhanced expression of IL-1β in the skin of the ear injected with MC/9 cells expressing R258W when compared with that observed with injection of MC/9 cells producing WT-Nlrp3 (Fig. 7 B). To determine whether the R258W-Nlrp3 mutation promotes vascular leakage, a hallmark of urticaria, we injected mice with MC/9 cells expressing WT and mutant Nlrp3 (R258W) in the ear skin and measured vascular leakage by Evans blue dye. Vascular leakage was significantly higher in the skin of mice injected with MC/9 cells expressing R258W-Nlrp3 than with cells expressing GFP alone or WT-Nlrp3 (Fig. 8, A and B). These results indicate that MCs expressing disease-associated Nlrp3 promote neutrophil recruitment and vascular leakage in the skin, two histological hallmarks of urticarial rash associated with CAPS.

DISCUSSION

MCs are widely distributed throughout vascularized tissues, where they are located near epithelial surfaces that are exposed to environmental cues, including the skin, airways, and gastrointestinal tract (28). MCs are known to promote inflammation and tissue remodeling in IgE-associated allergic disorders as well as to produce multiple cytokines, including IL-1β, in response to microbial stimuli, although the mechanisms involved remained unknown (29, 30). In this paper, we provide evidence that MCs express components of the inflammasome, and these factors are critical for the activation of caspase-1 and IL-1β secretion.

Our analysis revealed that Nlrp3 mutations associated with CAPS induce constitutive activation of the inflammasome in MCs, leading to dysregulated IL-1β production in the skin. These studies are consistent with a previous report that showed enhanced production of IL-1β in the skin of CAPS patients (31), although the cellular source of IL-1β was not investigated by the authors. We showed that transfer of MCs expressing the CAPS-associated Nlrp3 mutant induces perivascular neutrophil-rich inflammation in the mouse skin, which is the histological hallmark of the urticarial rash observed in CAPS patients. Collectively, these studies implicate MCs in inflammasome activation and the pathogenesis of IL-1β–mediated disease in the skin. Because MCs reside in multiples tissues and also participate in experimental models of arthritis (32) and encephalomyelitis (33–35), it is possible that these cells play a role in disease pathogenesis not only in

Published May 11, 2009

the skin but also in the joints and central nervous system, which are also major disease targets in CAPS patients (36). Further studies are needed to better understand the contribution of MCs to IL-1β–mediated disease in autoinflammatory syndromes associated with NLRP3 mutations.

The mechanism by which NLRP3 mutations cause inflammatory diseases is still poorly understood. Studies in vitro suggested that these mutations exert a gain-of-function effect, probably through the loss of a regulatory step associated with NLRP3 activation (6, 8). Consistently, mouse Nlrp3 mutants, corresponding to those observed in human CAPS, induced constitutive Asc-dependent NF-κB activation and IL-1β secretion. Notably, the increased production of IL-1β induced by CAPS-associated Nlrp3 mutants was abolished when their pyrin domain was deleted, which is in accordance with a critical role for that module in the interaction with caspase-1 and assembly of the inflammasome (6, 8).

As is the case with macrophages, production of mature IL-1β via the Nlrp3/Asc inflammasome in mouse MCs required two signals, LPS and ATP or R837. Although a main function of LPS is to induce pro–IL-1β production, LPS also promoted expression of *Nlrp3* in MCs, suggesting that LPS regulates inflammasome activation via several mechanisms in MCs. In macrophages, ATP-driven stimulation through the P2x7r is essential for caspase-1 proteolytic cleavage and IL-1β secretion via Nlrp3 (10, 19). The P2x7r forms a nonselective ion channel upon activation with ATP (19) and upon stimulation mediates K^+ efflux, which may be important for Nlrp3 activation (21). This ion channel mediated by P2x7r rapidly transitions to a pore-like structure by recruiting the pannexin-1 pore, which allows passage of molecules as large as 900 D (19). Therefore, it is possible, as it has been proposed for macrophages (37), that ATP promotes passage of microbial ligands such as LPS via pannexin-1 to trigger inflammasome activation in MCs. Consistently, ATP did not induce caspase-1 activation alone and triggered large pore formation in MCs, and this activity was blocked in P2x7r-deficient MCs. Unlike ATP, however, R837 did not induce large pore formation but elicited IL-1β secretion, at least in part, through P2x7r. The role of P2x7r in mediating IL-1β secretion in response to R837 stimulation is consistent with the observation that high K^+ extracellular medium blocked IL-1β secretion in MCs. Collectively, these results suggest that ATP and R837 may promote inflammasome activation via different mechanisms in MCs, although both stimuli require P2x7r and K^+ efflux for effective IL-1β secretion in MCs.

We observed a reduction in the amounts of TNF-α and IL-6 produced by MCs lacking *Nlrp3* compared with those from WT or Asc-deficient cells. The reason for this different regulation of cytokine secretion by Nlrp3 and Asc is unclear. One possibility is that Nlrp3 contributes to MC maturation in an Asc-independent manner. *Nlrp3* was first reported as an MC maturation–inducible gene (38) whose expression was

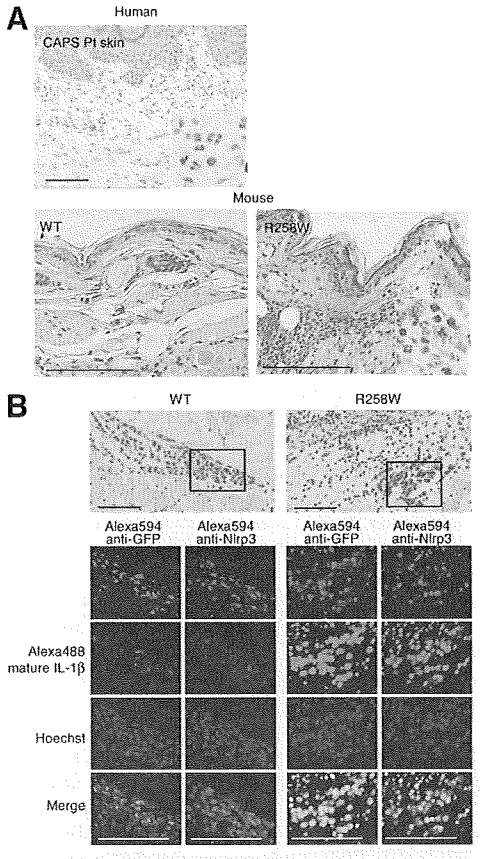

Figure 7. MCs expressing disease-associated Nlrp3 mutant induce neutrophil-rich inflammation in the mouse skin. 10^5 MC/9 cells expressing WT or mutant Nlrp3 (R258W) were injected into the skin of mice. (A, top) Representative images of the involved skin from a CAPS patient harboring an E567K *NLRP3* mutation. (bottom) Cross sections of mouse ears 36 h after injection with MC/9 cells. Tissue sections were stained with hematoxylin and eosin. Insets show a higher magnification demonstrating the presence of numerous neutrophils. Bars, 100 µm. (B) IL-1β expression in GFP^+ and $Nlrp3^+$ MC/9 cells. (bottom) Immunofluorescence images of mouse skin injected with MC/9 cells expressing WT or R258W-Nlrp3. Images were derived from tissues boxed in the top panels. All results are representative of at least three separate experiments. Bars, 50 µm.

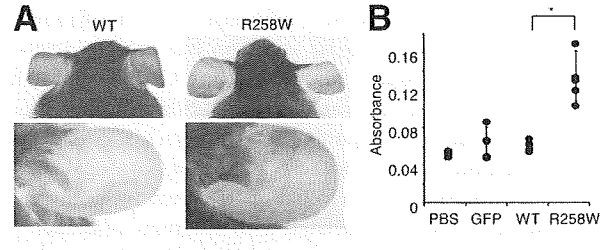

Figure 8. MCs expressing disease-associated Nlrp3 mutant induce vascular leakage in the mouse skin. Vascular leakage was analyzed by intravenous injection of 1% Evans blue solution 36 h after injection of mice with MC/9 cells expressing WT and mutant Nlrp3. (A, left) Mouse ears 30 min after dye injection. (B) Ears were collected, and vascular leakage was determined by absorbance at 620 nm in dye tissue extracts. Error bars represent means ± SD of results that are representative of at least three separate experiments. *, $P < 0.005$ between WT and R258W ($n = 4$ or 5 mice per group).

Published May 11, 2009

increased after the maturation into MCs with a connective tissue phenotype. Our BMCMCs were cultured with IL-3 and stem cell factor, which partially induce connective tissue–type maturation compared with the cells cultured with IL-3 alone. This possibility may explain, at least in part, why CAPS patients suffered from skin eruption but not asthma reaction or rhinitis, even though MCs in these tissues are likely to express the constitutively activated disease-associated NLRP3 mutation. However, no morphological and functional differences were observed between WT and Nlrp3-deficient MCs. Alternatively, Nlrp3 may directly or indirectly regulate cytokine production independently of the inflammasome in MCs.

CAPS-associated NLRP3 mutants constitutively produced IL-1β in MCs of the skin of patients and when injected into mouse tissues. However, it remains unclear why MCs with constitutive activation of the NLRP3 inflammasome produce mature IL-1β in the absence of LPS in patients given that microbial stimulation appears to be required for pro–IL-1β production. One possibility is that CAPS-associated NLRP3 mutants induce pro–IL-1β via constitutive activation of NF-κB induction, which is consistent with results found in the current work and also reported by others (26). Another possibility is that production of pro–IL-1β is induced by endogenous or environmental cues operating in the skin independently of NLRP3. Consistent with this model, the characteristic skin rash observed in CAPS and systemic inflammatory syndromes often develops within the first few weeks of life when the skin is first exposed to environmental factors. These may include exposure to small amounts of LPS and/or other microbial stimuli after birth. The observation that skin abnormalities in incontinentia pigmenti (MIM 308300), an X-linked dominant inherited disorder caused by the mutation of *NEMO*, a gene that encodes the regulatory component of the IκB kinase complex responsible for the activation of the NF-κB signaling pathway, commence at birth (39, 40) is also consistent with this possibility.

Urticarial rash associated with CAPS is usually nonpruritic and unresponsive to antihistamines. This clinical observation is in accordance with our observation that NLRP3 inflammasome activation induces IL-1β secretion but not degranulation in MCs. Nonetheless, MCs expressing CAPS-associated NLRP3 mutant promoted vascular permeability, a cellular response also induced by histamine release, which is critical for wheal formation in vivo. Because many cases of non-CAPS urticaria are unresponsive to histamine receptor antagonists, it is possible that skin rash associated with histamine resistance is mediated via inflammasome activation in MCs. Thus, understanding the pathophysiology of CAPS may provide critical insight into more common diseases such as antihistamine-refractory urticaria.

MATERIALS AND METHODS

Chemicals and reagents. Ultrapure LPS (*Escherichia coli* O55:B5), ATP, and MG-132 (Z-Leu-Leu-Leu-al) were purchased from Sigma-Aldrich. R837 (tlrl-imq) was purchased from InvivoGen. Abs for human cleaved IL-1β and IL-1β were purchased from Cell Signaling Technology, and human HLA-DR, -DP, -DQ (TAL.1B5) was purchased from Dako. Anti-human tryptase (G3) was provided by L. Schwartz (Virginia Commonwealth University, Richmond, VA). Anti-mouse IL-1β was purchased from R&D Systems. Abs for actin and cryopyrin were purchased from Santa Cruz Biotechnology, Inc., Tlr7 was purchased from Imgenex, and I-A^b (clone AF6-120.1) was purchased from BD. Anti-GFP was purchased from MBL International, and FITC- or Texas red–conjugated avidin was purchased from Invitrogen. Alexa Fluor 647–labeled anti-mouse IL-1β, Alexa Fluor 647–labeled anti-Ly-6G, and PE-labeled anti-CD45 were purchased from eBioscience.

Animals. *Nlrp3*$^{-/-}$, *Asc*$^{-/-}$, *Nlrc4*$^{-/-}$, and *P2x7r*$^{-/-}$ mice backcrossed at least eight times to C57BL6/J6 mice have been previously described (11, 41, 42). C57BL6/J6 mice were purchased from Crea Japan and housed in a pathogen-free facility. The animal studies were conducted under approved protocols by the Committee on the Use and Care of Animals of the University of Michigan and Chiba University.

Cultured MCs. The preparations of BMCMCs and FSMCs were previously described (24). The purity of MCs was confirmed by surface expression of CD45 and Kit, FITC-avidin labeling, and negative I-A^b expression (Fig. S2 A). Degranulation of MCs was assessed by β-hexosaminidase assay as previously described (24). Human MCs from cord blood were cultured as previously described (43).

Plasmid construction and retrovirus production. Plasmids to express mouse Nlrp3 have been previously described (31). Mutant Nlrp3 constructs corresponding to a human disease-associated mutation in the pEF-BOS vector were generated as previously described (18, 44). The ability of each construct to induce NF-κB activation was assessed with mouse Asc plasmid as previously described (18, 44). The retrovirus vector pMC-IRES-GFP (provided from T. Kitamura, University of Tokyo, Tokyo, Japan) containing Nlrp3 and its mutants was produced and introduced into Plat-E packaging cells with FuGENE6 (Roche). Immature BMCMCs cultured for 2 wk were incubated with retroviral supernatants for 15 h with 10 μg/ml polybrene (Sigma-Aldrich) (45). GFP-Nlrp3 fusion proteins were cloned into the pMX-IP vector and transfected into Plat-E cells. MC/9 cells were incubated with virus-containing supernatants and selected with 1.5 mg/ml puromycin.

Immunohistochemistry. Human and mouse skin biopsy samples were fixed with 4% paraformaldehyde, embedded in paraffin, and sectioned. Sections were stained with hematoxylin and eosin staining. Immunohistochemical staining was performed with primary Abs at the recommended concentrations followed by incubation with fluorescent dye–conjugated secondary Abs. Written informed consents were obtained from patients, according to the protocol of the institutional review board of Kyoto University Hospital and in accordance with the Declaration of Helsinki.

RT-PCR. Total RNA extracted from MCs (2×10^6) with TRIzol reagent (Invitrogen) was reverse transcribed and analyzed. The primers were as follows: *Nlrp3*, 5′-CACTTGGATCTAGCCACATC-3′ and 5′-AGCTCCAGCTTAAGGGAACTC-3′; *Asc*, 5′-ACTTGTCAGGGGATGAACTC-3′ and 5′-TGGTACTGTCCTTCAGTCAG-3′; *Casp1*, 5′-TACCTGGCAGGAATTCTGGA-3′ and 5′-ATGATCACCTTGGGCTTGTC-3′; *Il1b*, 5′-GCTTCCAAACCTTTGACCTG-3′ and 5′-CTGTTGTTTCCCAGGAAGAC-3′; *Tlr4*, 5′-CTGGCATCATCTTCATTGTCC-3′ and 5′-GCTTAGCAGCCATGTGTGTTCC-3′; *Tlr7*, 5′-CCACCAGACCTCTTGATTCC-3′ and 5′-TCCAGATGGTTCAGCCTACG-3′; *Gapdh*, 5′-CGGGAAGCTTGTCATCAATGG-3′ and 5′-GGCAGTGTGATGGCATGGATCTG-3′; *NLRP3*, 5′-AACAGCCACCTCACTTCCAG-3′ and 5′-GACGTAAGGCCAGAATTCAC-3′; *ASC*, 5′-TGGTCAGCTTCTACCTGGAG-3′ and 5′-TCCAGGCTGGTGTGAAACTG-3′; *CASP1*, 5′-GTACTTTCTTCCTTTCCAGCTC-3′ and 5′-TTCACATCTACGCTGTACCC-3′; and *IL1B*, 5′-TTCACATCTACGCTGTACCC-3′ and 5′-GTACTTTCTTCCTTTCCACCTC-3′. For real-time analysis, the mixture with Power SYBR Green PCR Master Mix (Applied Biosystems)

Published May 11, 2009

was amplified and analyzed with 7300 Real-Time PCR systems (Applied Biosystems).

Immunoblotting. Cell extracts were prepared in M-PER reagent (Thermo Fisher Scientific) in the presence of protease inhibitor cocktail (Thermo Fisher Scientific). Samples were denatured in 2× Laemmli sample buffer (Bio-Rad Laboratories) with 1 µl 2-ME. Lysates were separated by SDS-PAGE and transferred onto membranes (GE Healthcare). Membranes were incubated with an Ab against caspase-1, IL-1β, GFP, Tlr7, and actin, followed by horseradish peroxidase–conjugated Abs. Immunoreactive proteins were visualized with ECL detection reagents (GE Healthcare).

Cytokine ELISAs. Supernatants collected from 10^6 MCs/ml were measured for IL-1β (eBioscience), histamine (Invitrogen), TNF-α, and IL-6 (R&D Systems) by ELISA.

Neutrophil migration assay and histamine release. MC/9 cells stably expressing WT or mutant Nlrp3 (R258W) were suspended in PBS (10^7 cells/ml) and administrated i.p. (0.5 ml/mouse). 36 h after the injection, mice were sacrificed and the peritoneal cavity was lavaged with 2 ml PBS. After gentle massage, 1 ml of the peritoneal fluid was collected and centrifuged at 500 *g* for 5 min. Cells were stained for FACS analysis and the supernatant was used for histamine assay.

Evans blue dye injection assay. We modified the passive cutaneous anaphylaxis assay in mice as previously described (46). Right ears were injected intradermally with 10^5 cells in 0.1 ml saline and left ears were injected with saline as a control; 36 h later, mice were challenged with 0.5 ml saline containing 5 mg/ml Evans blue dye. Extravasation of Evans blue dye was monitored for 15 min, and ear biopsies were incubated at 63°C overnight in 700 µl formamide. Quantitative analysis of extracts was determined by measuring the absorbance at 620 nm.

Statistical analyses. All data are expressed as means ± SD. We accumulated the data for each condition from at least three independent experiments. We evaluated statistical significance with the Student's *t* test for comparisons between two mean values.

Online supplemental material. Fig. S1 shows the immunochemical staining of a CAPS patient's skin where tryptase-positive MCs, but not HLA-DR, -DP, -DQ–positive DCs or macrophages, were labeled with avidin and produced mature IL-1β. Fig. S2 shows the purity of BMCMCs and negative protein expression of Tlr7 on BMCMCs. Fig. S3 shows IL-1β, TNF-α, and IL-6 secretion from MCs in WT and Nlrc4-deficient mice. Fig. S4 shows a PCR analysis of the inflammasome components in mouse FSMCs that produced IL-1β, but did not show degranulation, in response to Nlrp3 activator. Fig. S5 shows a PCR analysis of the inflammasome components in human MCs that produced IL-1β in response to Nlrp3 activator. Fig. S6 shows the schematic structures of plasmids in pMX-IP retrovirus vector and the purity of MC/9 stably Nlrp3-GFP–expressing cells that did not show degranulation in response to Nlrp3 activator. Online supplemental material is available at http://www.jem.org/cgi/content/full/jem.20082179/DC1.

We would like to thank T. Kitamura for providing the pMC and pMX retrovirus system and Plat-E packaging cells, A. Fujisawa and H. Tanizaki for producing the plasmid for Nlrp3 disease-associated mutants, A. Niwa for help with human cord blood samples, S. Kagami and H. Umebayashi for the care of the patients, and G. Chen for critical review of the manuscript. We would also like to thank Y. Miyachi, T. Nakahata, and S. Shimada for encouragement and support of the work.

This work was supported in part by Grants-in-Aid for Scientific Research from the Ministry of Education, Culture, Sports, Science and Technology of Japan to N. Kambe (17790766 and 19591303), R. Nishikomori (19591249), M. Saito (195229), and H. Matsue (18390311 and 19659281), and grants from the National Institutes of Health (AI063331 and AR051790) to G. Núñez.

The authors have no conflicting financial interests.

Submitted: 29 September 2008
Accepted: 16 March 2009

REFERENCES

1. Nettis, E., A. Pannofino, C. D'Aprile, A. Ferrannini, and A. Tursi. 2003. Clinical and aetiological aspects in urticaria and angio-oedema. *Br. J. Dermatol.* 148:501–506.
2. Greaves, M. 2000. Chronic urticaria. *J. Allergy Clin. Immunol.* 105:664–672.
3. Sabroe, R.A., and M.W. Greaves. 2006. Chronic idiopathic urticaria with functional autoantibodies: 12 years on. *Br. J. Dermatol.* 154:813–819.
4. Kozel, M.M., and R.A. Sabroe. 2004. Chronic urticaria: aetiology, management and current and future treatment options. *Drugs.* 64:2515–2536.
5. Hull, K.M., N. Shoham, J.J. Chae, I. Aksentijevich, and D.L. Kastner. 2003. The expanding spectrum of systemic autoinflammatory disorders and their rheumatic manifestations. *Curr. Opin. Rheumatol.* 15:61–69.
6. Martinon, F., K. Burns, and J. Tschopp. 2002. The inflammasome: a molecular platform triggering activation of inflammatory caspases and processing of proIL-beta. *Mol. Cell.* 10:417–426.
7. Hoffman, H.M., J.L. Mueller, D.H. Broide, A.A. Wanderer, and R.D. Kolodner. 2001. Mutation of a new gene encoding a putative pyrin-like protein causes familial cold autoinflammatory syndrome and Muckle-Wells syndrome. *Nat. Genet.* 29:301–305.
8. Agostini, L., F. Martinon, K. Burns, M.F. McDermott, P.N. Hawkins, and J. Tschopp. 2004. NALP3 forms an IL-1beta-processing inflammasome with increased activity in Muckle-Wells autoinflammatory disorder. *Immunity.* 20:319–325.
9. Mariathasan, S., K. Newton, D.M. Monack, D. Vucic, D.M. French, W.P. Lee, M. Roose-Girma, S. Erickson, and V.M. Dixit. 2004. Differential activation of the inflammasome by caspase-1 adaptors ASC and Ipaf. *Nature.* 430:213–218.
10. Mariathasan, S., D.S. Weiss, K. Newton, J. McBride, K. O'Rourke, M. Roose-Girma, W.P. Lee, Y. Weinrauch, D.M. Monack, and V.M. Dixit. 2006. Cryopyrin activates the inflammasome in response to toxins and ATP. *Nature.* 440:228–232.
11. Kanneganti, T.D., N. Ozoren, M. Body-Malapel, A. Amer, J.H. Park, L. Franchi, J. Whitfield, W. Barchet, M. Colonna, P. Vandenabeele, et al. 2006. Bacterial RNA and small antiviral compounds activate caspase-1 through cryopyrin/Nalp3. *Nature.* 440:233–236.
12. Dostert, C., V. Petrilli, R. Van Bruggen, C. Steele, B.T. Mossman, and J. Tschopp. 2008. Innate immune activation through Nalp3 inflammasome sensing of asbestos and silica. *Science.* 320:674–677.
13. Eisenbarth, S.C., O.R. Colegio, W. O'Connor, F.S. Sutterwala, and R.A. Flavell. 2008. Crucial role for the Nalp3 inflammasome in the immunostimulatory properties of aluminium adjuvants. *Nature.* 453:1122–1126.
14. Li, H., S.B. Willingham, J.P. Ting, and F. Re. 2008. Cutting edge: inflammasome activation by alum and alum's adjuvant effect are mediated by NLRP3. *J. Immunol.* 181:17–21.
15. Saito, M., A. Fujisawa, R. Nishikomori, N. Kambe, M. Nakata-Hizume, M. Yoshimoto, K. Ohmori, I. Okafuji, T. Yoshioka, T. Kusunoki, et al. 2005. Somatic mosaicism of CIAS1 in a patient with chronic infantile neurologic, cutaneous, articular syndrome. *Arthritis Rheum.* 52:3579–3585.
16. Feldmann, J., A.M. Prieur, P. Quartier, P. Berquin, S. Certain, E. Cortis, D. Teillac-Hamel, A. Fischer, and G. de Saint Basile. 2002. Chronic infantile neurological cutaneous and articular syndrome is caused by mutations in CIAS1, a gene highly expressed in polymorphonuclear cells and chondrocytes. *Am. J. Hum. Genet.* 71:198–203.
17. Manji, G.A., L. Wang, B.J. Geddes, M. Brown, S. Merriam, A. Al-Garawi, S. Mak, J.M. Lora, M. Briskin, M. Jurman, et al. 2002. PYPAF1, a PYRIN-containing Apaf1-like protein that assembles with ASC and regulates activation of NF-kappa B. *J. Biol. Chem.* 277:11570–11575.
18. Saito, M., R. Nishikomori, N. Kambe, A. Fujisawa, H. Tanizaki, K. Takeichi, T. Imagawa, T. Iehara, H. Takada, T. Matsubayashi, et al. 2008. Disease-associated CIAS1 mutations induce monocyte death, revealing low-level mosaicism in mutation-negative cryopyrin-associated periodic syndrome patients. *Blood.* 111:2132–2141.
19. Ferrari, D., C. Pizzirani, E. Adinolfi, R.M. Lemoli, A. Curti, M. Idzko, E. Panther, and F. Di Virgilio. 2006. The P2X7 receptor: a key player in IL-1 processing and release. *J. Immunol.* 176:3877–3883.
20. Bulanova, E., V. Budagian, Z. Orinska, M. Hein, F. Petersen, L. Thon, D. Adam, and S. Bulfone-Paus. 2005. Extracellular ATP induces cytokine expression and apoptosis through P2X7 receptor in murine mast cells. *J. Immunol.* 174:3880–3890.

Published May 11, 2009

21. Pelegrin, P., and A. Surprenant. 2006. Pannexin-1 mediates large pore formation and interleukin-1beta release by the ATP-gated P2X7 receptor. *EMBO J.* 25:5071–5082.
22. Amer, A., L. Franchi, T.D. Kanneganti, M. Body-Malapel, N. Ozoren, G. Brady, S. Meshinchi, R. Jagirdar, A. Gewirtz, S. Akira, and G. Nunez. 2006. Regulation of *Legionella* phagosome maturation and infection through flagellin and host Ipaf. *J. Biol. Chem.* 281:35217–35223.
23. Franchi, L., A. Amer, M. Body-Malapel, T.D. Kanneganti, N. Ozoren, R. Jagirdar, N. Inohara, P. Vandenabeele, J. Bertin, A. Coyle, et al. 2006. Cytosolic flagellin requires Ipaf for activation of caspase-1 and interleukin 1beta in salmonella-infected macrophages. *Nat. Immunol.* 7:576–582.
24. Yamada, N., H. Matsushima, Y. Tagaya, S. Shimada, and S.I. Katz. 2003. Generation of a large number of connective tissue type mast cells by culture of murine fetal skin cells. *J. Invest. Dermatol.* 121:1425–1432.
25. Piccini, A., S. Carta, S. Tassi, D. Lasiglie, G. Fossati, and A. Rubartelli. 2008. ATP is released by monocytes stimulated with pathogen-sensing receptor ligands and induces IL-1beta and IL-18 secretion in an autocrine way. *Proc. Natl. Acad. Sci. USA.* 105:8067–8072.
26. Dowds, T.A., J. Masumoto, L. Zhu, N. Inohara, and G. Nunez. 2004. Cryopyrin-induced interleukin 1beta secretion in monocytic cells: enhanced activity of disease-associated mutants and requirement for ASC. *J. Biol. Chem.* 279:21924–21928.
27. Kagami, S., H. Saeki, Y. Kuwano, S. Imakado, and K. Tamaki. 2006. A probable case of Muckle-Wells syndrome. *J. Dermatol.* 33:118–121.
28. Galli, S.J., M. Grimbaldeston, and M. Tsai. 2008. Immunomodulatory mast cells: negative, as well as positive, regulators of immunity. *Nat. Rev. Immunol.* 8:478–486.
29. Supajatura, V., H. Ushio, A. Nakao, S. Akira, K. Okumura, C. Ra, and H. Ogawa. 2002. Differential responses of mast cell Toll-like receptors 2 and 4 in allergy and innate immunity. *J. Clin. Invest.* 109:1351–1359.
30. Lin, T.J., R. Garduno, R.T. Boudreau, and A.C. Issekutz. 2002. *Pseudomonas aeruginosa* activates human mast cells to induce neutrophil transendothelial migration via mast cell-derived IL-1 alpha and beta. *J. Immunol.* 169:4522–4530.
31. Hoffman, H.M., S. Rosengren, D.L. Boyle, J.Y. Cho, J. Nayar, J.L. Mueller, J.P. Anderson, A.A. Wanderer, and G.S. Firestein. 2004. Prevention of cold-associated acute inflammation in familial cold autoinflammatory syndrome by interleukin-1 receptor antagonist. *Lancet.* 364:1779–1785.
32. Nigrovic, P.A., B.A. Binstadt, P.A. Monach, A. Johnsen, M. Gurish, Y. Iwakura, C. Benoist, D. Mathis, and D.M. Lee. 2007. Mast cells contribute to initiation of autoantibody-mediated arthritis via IL-1. *Proc. Natl. Acad. Sci. USA.* 104:2325–2330.
33. Dietsch, G.N., and D.J. Hinrichs. 1989. The role of mast cells in the elicitation of experimental allergic encephalomyelitis. *J. Immunol.* 142:1476–1481.
34. Robbie-Ryan, M., M.B. Tanzola, V.H. Secor, and M.A. Brown. 2003. Cutting edge: both activating and inhibitory Fc receptors expressed on mast cells regulate experimental allergic encephalomyelitis disease severity. *J. Immunol.* 170:1630–1634.
35. Tanzola, M.B., M. Robbie-Ryan, C.A. Gutekunst, and M.A. Brown. 2003. Mast cells exert effects outside the central nervous system to influence experimental allergic encephalomyelitis disease course. *J. Immunol.* 171:4385–4391.
36. Neven, B., A.M. Prieur, and P. Quartier dit Maire. 2008. Cryopyrinopathies: update on pathogenesis and treatment. *Nat. Clin. Pract. Rheumatol.* 4:481–489.
37. Kanneganti, T.D., M. Lamkanfi, Y.G. Kim, G. Chen, J.H. Park, L. Franchi, P. Vandenabeele, and G. Nunez. 2007. Pannexin-1-mediated recognition of bacterial molecules activates the cryopyrin inflammasome independent of Toll-like receptor signaling. *Immunity.* 26:433–443.
38. Kikuchi-Yanoshita, R., Y. Taketomi, K. Koga, T. Sugiki, Y. Atsumi, T. Saito, S. Ishii, M. Hisada, T. Suzuki-Nishimura, M.K. Uchida, et al. 2003. Induction of PYPAF1 during in vitro maturation of mouse mast cells. *J. Biochem.* 134:699–709.
39. Berlin, A.L., A.S. Paller, and L.S. Chan. 2002. Incontinentia pigmenti: a review and update on the molecular basis of pathophysiology. *J. Am. Acad. Dermatol.* 47:169–187.
40. Nelson, D.L. 2006. NEMO, NFkappaB signaling and incontinentia pigmenti. *Curr. Opin. Genet. Dev.* 16:282–288.
41. Kanneganti, T.D., M. Body-Malapel, A. Amer, J.H. Park, J. Whitfield, L. Franchi, Z.F. Taraporewala, D. Miller, J.T. Patton, N. Inohara, and G. Nunez. 2006. Critical role for Cryopyrin/Nalp3 in activation of caspase-1 in response to viral infection and double-stranded RNA. *J. Biol. Chem.* 281:36560–36568.
42. Ozoren, N., J. Masumoto, L. Franchi, T.D. Kanneganti, M. Body-Malapel, I. Erturk, R. Jagirdar, L. Zhu, N. Inohara, J. Bertin, et al. 2006. Distinct roles of TLR2 and the adaptor ASC in IL-1beta/IL-18 secretion in response to *Listeria monocytogenes*. *J. Immunol.* 176:4337–4342.
43. Kambe, N., H. Hiramatsu, M. Shimonaka, H. Fujino, R. Nishikomori, T. Heike, M. Ito, K. Kobayashi, Y. Ueyama, N. Matsuyoshi, et al. 2004. Development of both human connective tissue-type and mucosal-type mast cells in mice from hematopoietic stem cells with identical distribution pattern to human body. *Blood.* 103:860–867.
44. Fujisawa, A., N. Kambe, M. Saito, R. Nishikomori, H. Tanizaki, N. Kanazawa, S. Adachi, T. Heike, J. Sagara, T. Suda, et al. 2007. Disease-associated mutations in CIAS1 induce cathepsin B-dependent rapid cell death of human THP-1 monocytic cells. *Blood.* 109:2903–2911.
45. Nishiyama, C., M. Nishiyama, T. Ito, S. Masaki, K. Maeda, N. Masuoka, H. Yamane, T. Kitamura, H. Ogawa, and K. Okumura. 2004. Overproduction of PU.1 in mast cell progenitors: its effect on monocyte- and mast cell-specific gene expression. *Biochem. Biophys. Res. Commun.* 313:516–521.
46. Kabu, K., S. Yamasaki, D. Kamimura, Y. Ito, A. Hasegawa, E. Sato, H. Kitamura, K. Nishida, and T. Hirano. 2006. Zinc is required for Fc epsilon RI-mediated mast cell activation. *J. Immunol.* 177:1296–1305.
47. Duncan, J.A., D.T. Bergstralh, Y. Wang, S.B. Willingham, Z. Ye, A.G. Zimmermann, and J.P. Ting. 2007. Cryopyrin/NALP3 binds ATP/dATP, is an ATPase, and requires ATP binding to mediate inflammatory signaling. *Proc. Natl. Acad. Sci. USA.* 104:8041–8046.

The Journal of Immunology

T Cell Leukemia/Lymphoma 1 and Galectin-1 Regulate Survival/Cell Death Pathways in Human Naive and IgM + Memory B Cells through Altering Balances in Bcl-2 Family Proteins

Siamak Jabbarzadeh Tabrizi, Hiroaki Niiro, Mariko Masui, Goichi Yoshimoto, Tadafumi Iino, Yoshikane Kikushige, Takahiro Wakasaki, Eishi Baba, Shinji Shimoda, Toshihiro Miyamoto, Toshiro Hara and Koichi Akashi

J. Immunol. 2009;182;1490-1499
http://www.jimmunol.org/cgi/content/full/182/3/1490

The Journal of Immunology is published twice each month by The American Association of Immunologists, Inc., 9650 Rockville Pike, Bethesda, MD 20814-3994.

Print ISSN: 0022-1767 Online ISSN: 1550-6606.

T Cell Leukemia/Lymphoma 1 and Galectin-1 Regulate Survival/Cell Death Pathways in Human Naive and IgM$^+$ Memory B Cells through Altering Balances in Bcl-2 Family Proteins[1]

Siamak Jabbarzadeh Tabrizi,* Hiroaki Niiro,[2†] Mariko Masui,[‡] Goichi Yoshimoto,[†] Tadafumi Iino,[§] Yoshikane Kikushige,[†] Takahiro Wakasaki,[¶] Eishi Baba,[†] Shinji Shimoda,[†] Toshihiro Miyamoto,[‡] Toshiro Hara,* and Koichi Akashi[†§]

BCR signaling plays a critical role in purging the self-reactive repertoire, or in rendering it anergic to establish self-tolerance in the periphery. Differences in self-reactivity between human naive and IgM$^+$ memory B cells may reflect distinct mechanisms by which BCR signaling dictates their survival and death. Here we demonstrate that BCR stimulation protected naive B cells from apoptosis with induction of prosurvival Bcl-2 family proteins, Bcl-x_L and Mcl-1, whereas it rather accelerated apoptosis of IgM$^+$ memory B cells by inducing proapoptotic BH3-only protein Bim. We found that BCR-mediated PI3K activation induced the expression of Mcl-1, whereas it inhibited Bim expression in B cells. Phosphorylation of Akt, a downstream molecule of PI3K, was more sustained in naive than IgM$^+$ memory B cells. Abundant expression of T cell leukemia/lymphoma 1 (Tcl1), an Akt coactivator, was found in naive B cells, and enforced expression of Tcl1 induced a high level of Mcl-1 expression, resulting in prolonged B cell survival. In contrast, Galectin-1 (Gal-1) was abundantly expressed in IgM$^+$ memory B cells, and inhibited Akt phosphorylation, leading to Bim up-regulation. Enforced expression of Gal-1 induced accelerated apoptosis in B cells. These results suggest that a unique set of molecules, Tcl1 and Gal-1, defines distinct BCR signaling cascades, dictating survival and death of human naive and IgM$^+$ memory B cells. *The Journal of Immunology,* **2009, 182: 1490–1499.**

Primary human peripheral B cells are made up of heterogeneous subpopulations that include a high proportion of memory B cells compared with those in rodents. Due to the advantage conferred by the usefulness of CD27 as a memory marker in humans, peripheral B cells are divided into at least three distinct subsets: naive (IgM$^+$CD27$^-$), IgM$^+$ memory (IgM$^+$CD27$^+$), and switched memory (IgG$^+$A$^+$CD27$^+$) B cells (1). Of particular interest are IgM$^+$ memory B cells in that they do not exist in mice and could develop through the novel germinal center-independent pathways and express somatically mutated IgM Abs (2). To date, IgM$^+$ memory B cells have been proposed to be circulating splenic marginal zone (MZ)[3] B cells and to play a critical role in the protection against encapsulated organisms (2, 3). Although in vivo function of IgM$^+$ memory B cells is becoming evident (4), the molecular mechanisms of activation of this subset remain poorly characterized.

Due to random rearrangements of the subunits of a functional BCR from genomic cassettes, a large proportion of developing human B cells in the bone marrow express self-reactive BCRs, but most of these potentially noxious BCRs are purged from the repertoire at several checkpoints in the bone marrow and the periphery (5). Nevertheless, up to 20% of mature naive B cells in normal peripheral blood still express low-affinity self-reactive BCRs (5). In sharp contrast, IgM$^+$ memory B cells isolated from normal donors are devoid of such self-reactive BCRs (6). These findings suggest a distinct homeostatic control of human naive and IgM$^+$ memory B cells.

BCR transmits the signals that are critical for both the elimination of self-reactive repertoire and the expansion of pathogen-specific repertoire. Upon BCR ligation by Ags, Lyn and Syk protein tyrosine kinases are initially activated. Syk propagates the signal by phosphorylating downstream signaling molecules. This results in activation of key signaling intermediates PI3K and phospholipase C (PLC)γ2. PI3K activates Akt kinase, which is critical for B cell survival (7). PLCγ2 activation leads to the release of intracellular Ca^{2+} and protein kinase C activation, which in turn cause activation of MAPK family kinases (ERK, JNK, and p38 MAPK) and transcription factors including NF-κB and NF-AT. These outputs subsequently connect with further-downstream molecules responsible for determining B cell fates such as survival, growth, and differentiation.

*Department of Pediatrics, Graduate School of Medical Sciences, Kyushu University, Fukuoka, Japan; †Department of Medicine and Biosystemic Science, Graduate School of Medical Sciences, Kyushu University, Fukuoka; ‡Center for Cellular and Molecular Medicine, Kyushu University Hospital, Fukuoka, Japan; §Department of Cancer Immunology and AIDS, Dana-Farber Cancer Institute, MA 02115; and ¶Department of Otorhinolaryngology, Graduate School of Medical Sciences, Kyushu University, Fukuoka, Japan

Received for publication August 7, 2008. Accepted for publication November 15, 2008.

The costs of publication of this article were defrayed in part by the payment of page charges. This article must therefore be hereby marked *advertisement* in accordance with 18 U.S.C. Section 1734 solely to indicate this fact.

[1] This work was supported in part by a Grant-in-Aid from the Ministry of Education, Culture, Sports, Science, and Technology in Japan (to S.J.T., H.N., T.H., and K.A.).

[2] Address correspondence and reprint requests to Dr. Hiroaki Niiro, Department of Medicine and Biosystemic Science, Graduate School of Medical Sciences, Kyushu University, 3-1-1 Maidashi, Higashi-ku, Fukuoka 812-8582, Japan. E-mail address: hniiro@med.kyushu-u.ac.jp

[3] Abbreviations used in this paper: MZ, marginal zone; Gal-1, galectin-1; Tcl1, T cell leukemia/lymphoma 1; PLC, phospholipase C; h, human; EGFP, enhanced GFP; CLL, chronic lymphocytic leukemia; BAFF, B cell-activating factor of the TNF family.

The Bcl-2-regulated pathway plays a critical role in BCR-induced survival and death (8, 9). The Bcl-2 family proteins fall into three subgroups: the first subgroup including Bcl-2, Bcl-x_L, and Mcl-1 inhibits some apoptotic pathways; the second subgroup including Bax and Bak directly induces apoptosis by promoting cytochrome *c* release from the mitochondria; the third subgroup, called BH3-only proteins, consists of at least eight mammalian proapoptotic proteins and is activated in a stimulus-specific, as well as a cell type-specific, manner. Among Bcl-2 family proteins, a BH3-only protein Bim is particularly important in controlling lymphocyte apoptosis. Bim deficiency causes a substantial expansion of autoreactive B cells leading to autoimmune diseases (10). B cells lacking Bim are refractory to BCR-induced apoptosis (10). Bim preferentially binds anti-apoptotic Mcl-1 (11, 12). Conditional knockout of Mcl-1 causes premature death of immature and mature B cells (12), suggesting a pivotal role of Mcl-1 in B cell survival. Based on these findings, tipping the balance between Mcl-1 and Bim expression may be a critical determinant for B cell survival and death. To date, little is known about how BCR signaling dictates the survival and death of human B cell subsets via the Bcl-2-regulated pathway.

In this study, we demonstrate that BCR stimulation rescued naive B cells from apoptosis with Bcl-x_L and Mcl-1 induction, whereas it rather accelerated apoptosis of IgM^+ memory B cells with Bim induction. Sustained Akt activation in naive but not IgM^+ memory B cells appears to be critical for reciprocal expression pattern of these Bcl-2 family proteins. Moreover, we demonstrate that T cell leukemia/lymphoma 1 (Tcl1) and galectin-1 (Gal-1), abundantly expressed in naive and IgM^+ memory B cells, respectively, play a crucial role in regulating Akt activation, thereby affecting their survival and death via the Bcl-2-regulated pathway.

Materials and Methods

Reagents

PE-Cy5-conjugated mouse anti-human (h) CD3, -hCD4, -hCD8, -hCD11b, -hCD14, -hCD56, and -human glycophorin A mAbs; FITC-conjugated mouse anti-hCD19, -hCD69, -hCD86, -hCD95 mAbs; and PE-conjugated mouse anti-hCD27 mAb were purchased from BD Immunocytometry. FITC-conjugated goat anti-hIgM, -hIgD, -hIgG, -hIgA, rabbit anti-hGal-1 sera and recombinant hGal-1 were obtained from MBL. Goat anti-hIgM and IgG/IgA/IgM $F(ab')_2$ fragments were purchased from Jackson ImmunoResearch Laboratories. Rabbit anti-human phospho-ZAP70/Syk, anti-human phospho-PLCγ2 (Y1217), anti-human phospho-JNK, anti-human phospho-ERK, anti-human phospho-Akt, anti-human Bim, anti-human Tcl1 sera, and rabbit anti-human phospho-p85/p70 S6K, anti-human phospho-NF-κB p65, and anti-human Bcl-x_L mAbs were from Cell Signaling Technology. Mouse anti-β-actin mAb and rabbit anti-human Mcl-1 sera were from Sigma-Aldrich. A PI3K inhibitor (Ly294002) was purchased from Calbiochem (EMD Biosciences).

Isolation and culture of B cell subsets

Human PBMCs were separated from buffy coats kindly provided by Fukuoka Red Cross Blood Center (Chikushino, Japan). The buffy coats originate from kind whole blood donations of RBC transfusion by healthy volunteers (age range, 18–55 years). Informed consent was obtained from all subjects. B cells were isolated with Dynabeads M450 CD19 and DETACHaBEAD CD19 (Dynal Biotech) according to the manufacturer's instructions. Isolated B cells exhibited >99.5% viability confirmed by trypan blue exclusion and >95% purity by flow cytometry. Cells were further purified by cell sorting using a FACSAria (BD Biosciences). A representative sample of human B cell subsets is shown in Fig. 1*A*. Cells were stained with PE-Cy5-conjugated anti-hCD3, -hCD4, -hCD8, -hCD11b, -hCD14, -hCD56, -human glycophorin A; FITC-conjugated anti-human IgG; FITC-conjugated anti-human IgA; and PE-conjugated anti-hCD27 to obtain naive ($IgG^-A^-CD27^-$), IgM^+ memory ($IgG^-A^-CD27^+$), and switched memory (IgG^+/IgA^+CD27^+) B cells. Isolated B cell subsets exhibited >95% viability confirmed by trypan blue exclusion and >99% purity by flow cytometry (Fig. 1*B*). Cells were cultured at 1×10^6 cells/ml in a flat-bottom 96-well microtiter plate in complete RPMI 1640 supplemented with 10% FCS. Preliminary experiments showed that trace levels of phosphorylation of BCR signaling molecules are observed in B cell subsets immediately after purification probably due to mechanical stress. The cells were thus rested for a couple of hours and used for further analysis throughout the study. Consistent with a previous study (2), IgM^+ memory B cells exhibited a slightly higher level of IgM and a slightly lower level of IgD than did naive B cells (Fig. 1*C*). Absence of surface expression of CD95, CD86, and CD69, representative activation markers, in both subsets before stimulation, suggests that these cells are rested (Fig. 1*C*).

Expression constructs and transient transfection of human B subsets

Constructs encoding human Tcl1- or Gal-1-enhanced GFP (EGFP) fusion proteins (pEGFP-Tcl1 or -Gal-1) were generated by inserting sequence encoding the full-length protein into the pEGFP-N3 vector (Clontech). Transient transfections of B cell subsets with pEGFP-Tcl1 or pEGFP-Gal-1 were conducted using the Nucleofector protocol from AMAXA Biosystems. Cells (1×10^6) were suspended in 100 μl of Nucleofector solution with 5 μg of plasmid DNA and then electroporated using program U-15. Cells were transferred to 2.5 ml of medium containing 15% FCS and harvested 24 h after transfection. The transfection efficiency ranges between 20 and 30% for each experiment.

Annexin V staining

After culture, cells ($1–2 \times 10^5$) were washed twice with PBS and then suspended in 85 μl of binding buffer (MBL) containing Ca^{2+}. Cell suspension supplemented with 10 μl of annexin V-FITC or -PE (MBL) and 5 μg of propidium iodide or 1 μg of 7-aminoactinomycin D was incubated at room temperature for 15 min in the dark. Subsequently, 600 μl of binding buffer were added, and the percentage of early apoptotic cells was measured using flow cytometry.

Mitochondria membrane potential

Assessment of mitochondria membrane potential was performed using Mitotracker Red CMXRos (Invitrogen). Cells were incubated in 50 nM Mitotracker Red at 37°C for 1 h in the dark. Flow cytometric analysis (50,000 events/sample) was performed on FACSCalibur (BD Biosciences). Cell debris was electronically gated out based on the forward scatter. Data were further analyzed using FlowJo software.

Measurement of intracellular free calcium

Cells were washed with RPMI 1640 containing 10% FCS and adjusted at 1×10^6 cells/ml. After incubation at 37°C for 15 min, 1 μg/ml fluo-4-acetoxymethyl esterM (Dojindo) was added, and the cells were incubated for a further 30–45 min with resuspension every 15 min. The cells were centrifuged and resuspended in RPMI 1640 at 2×10^6 cells/ml. The cells were stimulated with anti-IgM (20 μg/ml), and the fluorescence intensity of intracellular fluo 4 was monitored and analyzed using flow cytometry.

Western blot analysis

Unstimulated or stimulated cells (1×10^6) were lysed as described (13). Lysates were then denatured in an equal volume of 2× SDS sample buffer, resolved by a 10% SDS-PAGE gel and electrotransferred to nitrocellulose membranes in non-SDS-containing transfer buffer (25 mM Tris, 0.2 M glycine, 20% methanol, pH 8.5). Western blotting was performed with anti-phospho-Syk (1/2,000), anti-phospho-PLCγ2 (1/2,000), anti-phospho-p85/p70 S6 kinase (1/2,000), anti-phospho-JNK (1/2,000), anti-phospho-ERK (1/2,000), anti-phospho-Akt (1/2,000), anti-phospho-p65 NF-κB (1/2,000), anti-Bim (1/2,000), anti-Bcl-x_L (1/2,000), anti-Mcl-1 (1/5,000), anti-Tcl1 (1/2,000), anti-Gal-1 (1/2,000), and anti-β-actin (1/5,000) followed by a 1/15,000 dilution of anti-rabbit or anti-mouse HRP-conjugated IgG (Jackson ImmunoResearch Laboratories). Blots were developed with ECL plus kit (Amersham Biosciences). The chemiluminescence intensity was monitored with a laser3000 (FujiFilm) instrument. We quantitated band intensity of the proteins using ImageGauge software (FujiFilm) and normalized their expression in reference to β-actin levels. Using these normalized data, relative expression is subsequently calculated as fold changes in protein expression compared with the controls.

Quantitative real-time PCR

Total RNA was extracted from sorted human B cell subsets using Isogen reagent (Nippon Gene) and treated with DNase I (Invitrogen) to remove contaminating genomic DNA. First-strand cDNA was synthesized using a

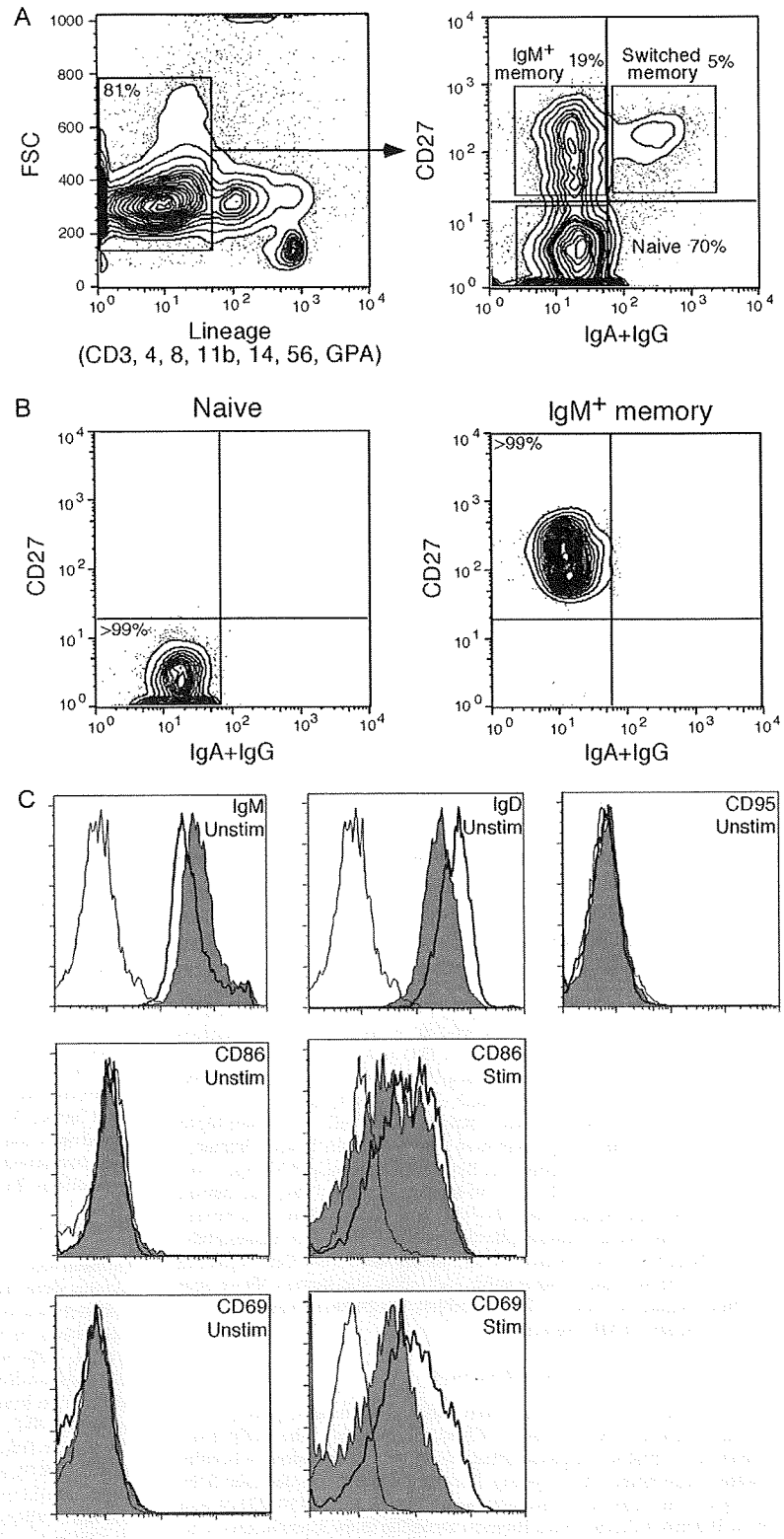

FIGURE 1. Isolation of purified human peripheral B cell subsets. *A*, Phenotypic analysis of B cell subsets in human peripheral blood. Donor B cells were purified by staining with Abs to CD3, CD4, CD8, CD11b, CD14, CD56, and glycophorin A (GPA) and were then evaluated by flow cytometry. B cell subsets were identified according to surface IgG/IgA and CD27 expression: $IgG^-A^-CD27^-$ B cells (naive), $IgG^-A^-CD27^+$ B cells (IgM^+ memory), and $IgG^+A^+CD27^+$ B cells (switched memory). Data are presented as density plots. *B*, Highly purified B cell subsets were separated after cell sorting. *C*, Surface marker expression in human B cell subsets. Purified B cell subsets before (Unstim) and after stimulation (Stim) with 20 μg/ml $F(ab')_2$ goat anti-hIgM (36 h) were analyzed separately for IgM, IgD, CD95, CD86, and CD69 surface expression. Bold line, Naive B cells; gray area, IgM^+ memory B cells; thin line, isotype control line. These results are representative of peripheral blood samples from more than 10 different donors.

QuantiTect reverse transcription kit (Qiagen). Quantitative real-time PCR was conducted in the ABI Prism 7700 Sequence Detector (Applied Biosystems). Reactions were performed in triplicate wells in 96-well plates. TaqMan target mixes for Bim, Bcl-x_L, Mcl-1, Tcl1, and Gal-1 were purchased from Applied Biosystems. 18S rRNA was separately amplified in the same plate to be used as an internal control for variances in the amount of cDNA in PCR. Collected data were analyzed with Sequence Detector software (Applied Biosystems). Data were expressed as a fold change in gene expression relative to those from unstimulated naive B cells.

Intracellular flow cytometry

After two washings with PBS containing 1% FCS, 5×10^5 cells were placed in a 96-well microtiter plate. Cells were resuspended with 50 μl of medium plus 50 μl of fixation buffer (BD Biosciences) and incubated for 10 min at 37°C. After washing again with PBS containing 1% FCS, cells were suspended with 50 μl of saponin permeabilization buffer (BD Biosciences) and spun down. The cell pellet was incubated with primary Abs (anti-human Mcl-1 or Bim) in saponin buffer at room temperature for

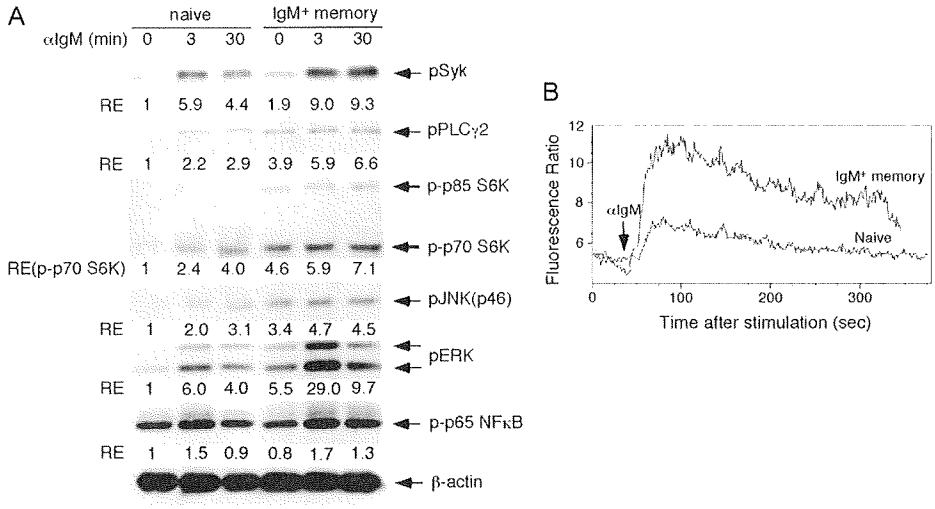

FIGURE 2. BCR signaling profiles of naive and IgM$^+$ memory B cells at early time points. *A*, B cell subsets were stimulated with 20 μg/ml F(ab')$_2$ goat anti-hIgM for the indicated time intervals. Cell lysates were subsequently separated on an 8% or 10% SDS-PAGE gel, and analyzed by Western blotting with anti-phospho-Syk, -PLCγ2, -JNK, -ERK sera, and anti-phospho-p70/85 S6K, -p65 NF-κB mAb and anti-β-actin mAb. Results are representative of three independent experiments. RE, Relative expression. *B*, Ca^{2+} mobilization in naive and IgM$^+$ memory B cells. Intracellular free calcium levels in fluo-4-acetoxymethyl ester-loaded cells were monitored using flow cytometry, after cells were stimulated with 20 μg/ml F(ab')$_2$ goat anti-hIgM. Results are representative of five independent experiments.

30–45 min. After a washing with PBS containing 1% FCS, cell were incubated with PE-conjugated donkey anti-rabbit IgG (Jackson Immuno-Research Laboratories) at room temperature for 30–45 min. Cells were washed one more time with PBS containing 1% FCS and analyzed at low flow rate on a FACSCalibur. B cell population was identified on its forward and side scatter distribution, and 15,000 cell events were analyzed for mean fluorescence using FlowJo software.

Results

Early BCR signaling is exaggerated in IgM$^+$ memory but not naive B cells

BCR signaling is critical for B cell fate decisions such as B cell survival, growth, and differentiation (14). We first tested whether the profile of early BCR signaling is different between naive and IgM$^+$ memory B cells. Phosphorylation of Syk, one of the earliest events in BCR signaling, was more pronounced in IgM$^+$ memory B cells (Fig. 2*A*). Two enzymes, PI3K and PLCγ2, function as critical mediators downstream of Syk activation in B cells (15). Phosphorylation of p85/p70 S6K, a downstream molecule of PI3K, and PLCγ2, was more pronounced in IgM$^+$ memory B cells (Fig. 2*A*). Activated PLCγ2 converts phosphatidylinositol 4,5-bisphosphate into IP3 and diacyl glycerol, the former of which is critical for calcium flux in B cells (14). Consistent with PLCγ2 phosphorylation, BCR-induced calcium flux was higher in IgM$^+$ memory B cells (Fig. 2*B*). Calcium flux and diacyl glycerol led to activation of NF-κB and MAPKs such as JNK and ERK. Phosphorylation of JNK and ERK was more pronounced in IgM$^+$ memory B cells, whereas p65 NF-κB phosphorylation was comparable in both subsets (Fig. 2*A*). Taken together, during the early phase of BCR activation, downstream signaling is pronounced especially in IgM$^+$ memory B cells as compared with naive B cells.

BCR stimulation rescues naive but not IgM$^+$ memory B cells from apoptosis

Following anti-IgM stimulation alone, naive and IgM$^+$ memory B cells did not either divide or release Igs in the culture (data not shown), suggesting that BCR signaling alone is not sufficient to induce the growth and differentiation of human B cell subsets. We then tested whether the BCR signaling affects the survival and death of naive and IgM$^+$ memory B cells. In the absence of stimuli, a considerable fraction of purified naive and IgM$^+$ memory B cells underwent apoptotic cell death within 2 days in vitro (Fig. 3*A*). Spontaneous cell death was more pronounced in naive B cells than in IgM$^+$ memory B cells. BCR stimulation, however, significantly rescued naive B cells from apoptosis, whereas IgM$^+$ memory B cells were not rescued (Fig. 3, *A* and *B*). Thus, BCR signaling can protect naive, but not IgM$^+$ memory B cells from apoptotic cell death.

Mitochondrial perturbations including cytochrome *c* release and inner membrane depolarization correlate with BCR-induced apoptosis (16). We thus tested whether BCR-induced depolarization of the mitochondrial inner membrane could be altered in naive and IgM$^+$ memory B cells. High levels of mitochondrial membrane potential were observed in both subsets immediately after sorting, indicating their highly viable state (Fig. 3*C*, *a* and *d*). A 2-day culture of these subsets without stimuli caused a remarkable decrease in mitochondrial membrane potential (Fig. 3*C*, *b* and *e*). BCR stimulation for 2 days, however, partially abrogated the loss of mitochondrial membrane potential in naive, but not IgM$^+$ memory B cells (Fig. 3*C*, *c* and *f*). Thus, BCR signaling rescues the B cell apoptosis pathway upstream of mitochondrial damage in naive, but not IgM$^+$ memory B cells.

BCR stimulation induces anti-apoptotic Mcl-1 in naive B cells, whereas it induces proapoptotic Bim in IgM$^+$ memory B cells at the protein level

Bcl-2 family proteins are the primary regulators of mitochondrial membrane integrity and play a vital role in the control of apoptosis (9). We tested whether BCR signaling affects gene expression of Bim, Bcl-x_L, and Mcl-1 in naive and IgM$^+$ memory B cells (Fig. 4*A*). Bcl-x_L mRNA expression was induced after BCR stimulation in both subsets, and such induction was more pronounced in naive B cells. In contrast, the expression level of Bim mRNA was slightly higher in IgM$^+$ memory B cells irrespective of BCR stimulation. Mcl-1 mRNA expression was not significantly changed in both subsets. We next tested whether BCR signaling affects protein

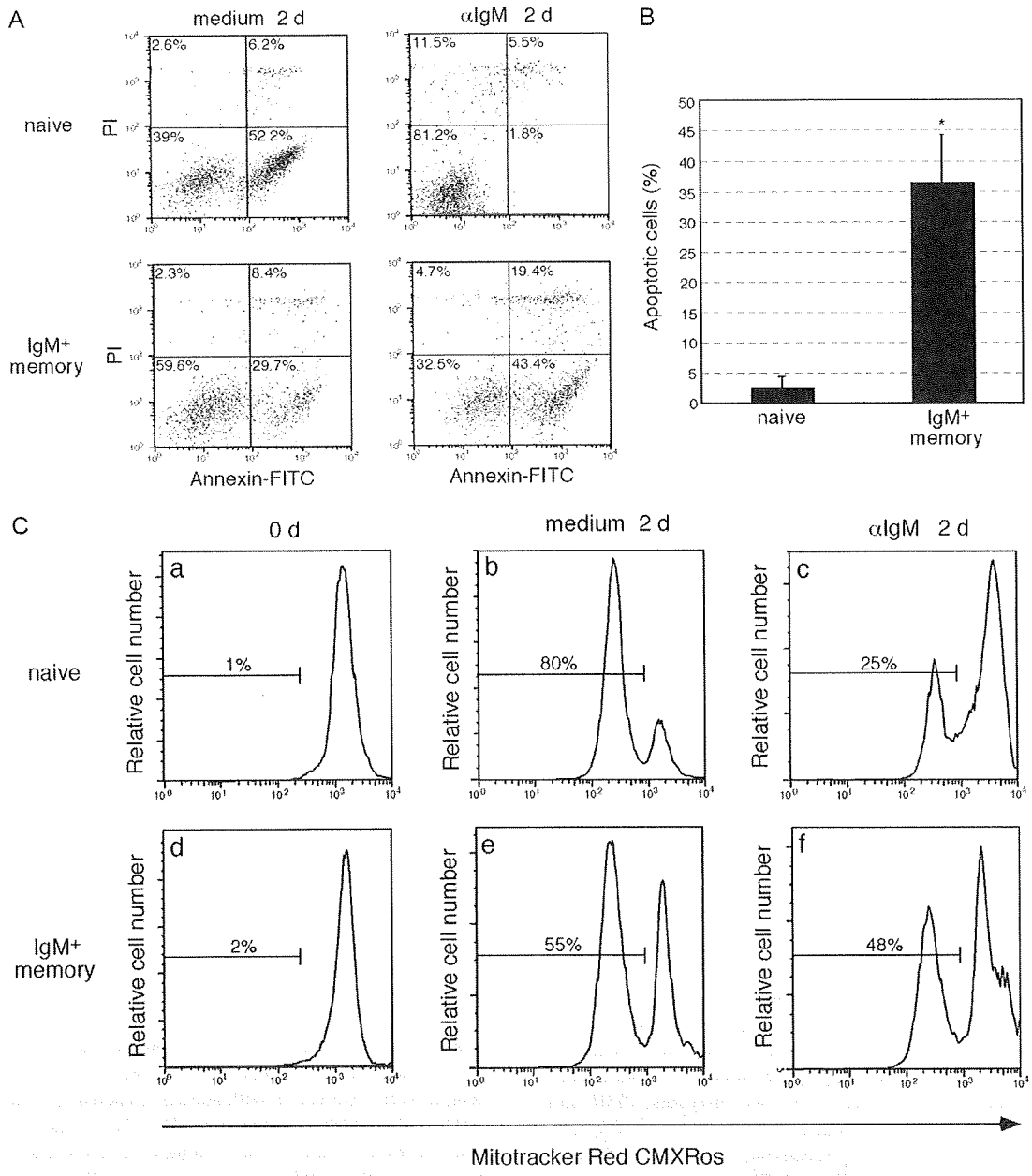

FIGURE 3. BCR-induced apoptosis in B cell subsets. *A*, Naive and IgM^+ memory B cells were incubated in the absence or presence of 20 μg/ml $F(ab')_2$ goat anti (α)-hIgM. After 2 days (2 d) of culture, cells were double-stained with FITC-labeled annexin V and propidium iodide (PI) and analyzed using flow cytometry. Apoptotic cells are visible as annexin V-positive population, both propidium iodide negative (early apoptosis) and propidium iodide positive (late apoptosis). The results shown are representative of three independent experiments. *B*, Percentage apoptosis of B cell subsets after BCR stimulation. The data are shown as the mean SD of six independent experiments. *, $p < 0.01$. *C*, BCR-induced mitochondrial inner membrane depolarization in B cell subsets. Naive and IgM^+ memory B cells were treated for 2 days with either medium or 20 μg/ml $F(ab')_2$ goat anti-human IgM. Percentages of Mitotracker Red $CMXRos^{low}$ cells are shown. Data obtained from cells immediately after isolation are also shown. Results are representative of three independent experiments.

expression of Bim, Bcl-x_L, and Mcl-1 in naive and IgM^+ memory B cells (Fig. 4*B*). Three isoforms (Bim-EL, Bim-L, and Bim-S) are expressed in various cell types, including lymphocytes (17). In the absence of stimuli, Bim-EL was weakly expressed in both subsets, but in IgM^+ memory B cells BCR stimulation induced all of three Bim isoforms at the level higher than those in naive B cells. On the other hand, the expression level of anti-apoptotic proteins Bcl-x_L and Mcl-1 was higher in naive B cells after BCR stimulation. Given that the difference in expression levels of surface IgM between two subsets (Fig. 1*C*) might cause these phenomena, we tested Mcl-1 expression in naive and IgM^+ memory B cells using titrated doses of anti-IgM Ab. Higher levels of Mcl-1 in naive B cells were observed at all doses of anti-IgM tested (Fig. 4*C*). Collectively, these results suggest that after BCR stimulation, anti-apoptotic Bcl-x_L and Mcl-1 are predominantly expressed in naive B cells, whereas the proapoptotic protein Bim was more abundantly expressed in IgM^+ memory B cells. The discrepancy of mRNA and protein levels strongly suggests the existence of post-transcriptional regulation of Bim and Mcl-1 expression in both subsets.

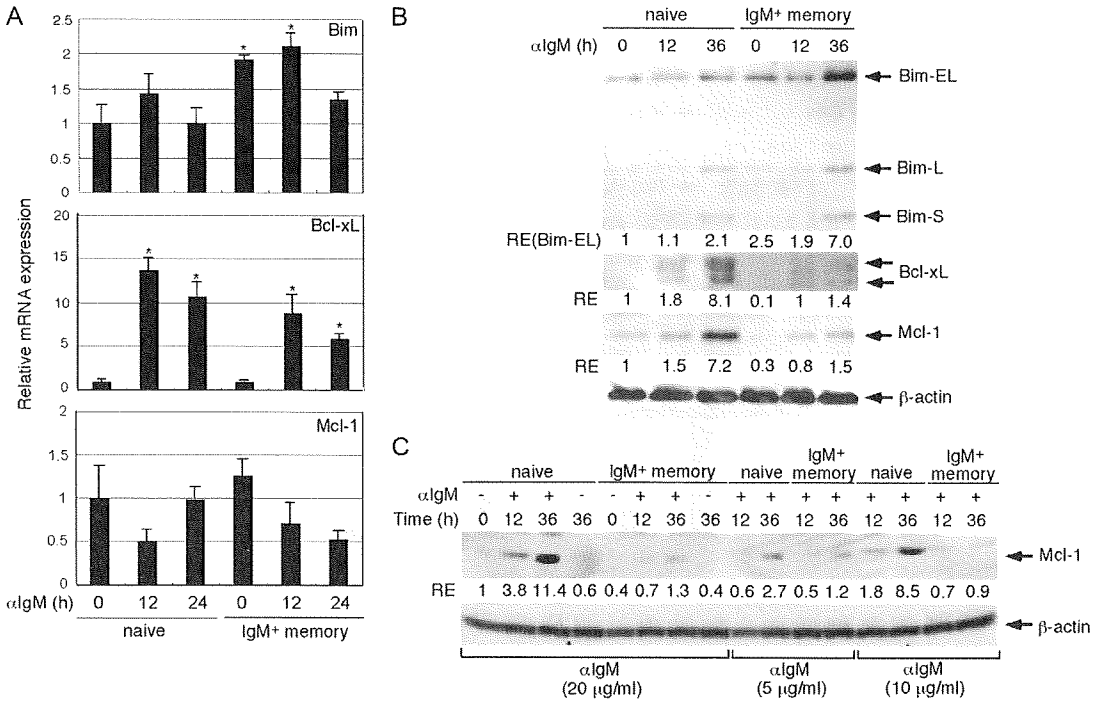

FIGURE 4. BCR-induced expression of Bcl-2 family proteins in B cell subsets. Naive and IgM^+ memory B cells were incubated for the indicated time periods in the absence or presence of 20 mg/ml $F(ab')_2$ goat anti (α)-hIgM. *A*, Quantitation of Bim, Bcl-x_L, and Mcl-1 mRNA by real-time PCR in B cell subsets. Data are normalized to the expression of 18S rRNA. Results are representative of three independent experiments. *, $p < 0.01$. *B*, Cell lysates were separated on a 12.5% SDS-PAGE gel, and analyzed by Western blotting with anti-Bim and -Mcl-1 sera and anti-Bcl-x_L and -β-actin mAb. The results shown are representative of five independent experiments. RE, Relative expression. *C*, Effect of a titrated dose of anti-IgM on Mcl-1 induction in B cell subsets. Results are representative of three independent experiments. RE, relative expression.

PI3K activation plays a role in reciprocal regulation of Mcl-1 and Bim protein in B cell subsets

A previous report suggests a critical role of the PI3K pathway in Mcl-1 expression (18). We tested an effect of a selective PI3K inhibitor Ly294002 on BCR-induced Mcl-1 expression in naive B cells (Fig. 5*A*). Treatment of cells with Ly294002 strongly inhibited Mcl-1 induction in naive B cells, suggesting a critical role of PI3K activity in Mcl-1 expression in naive B cells. In contrast, Ly294002 treatment induced the expression of Bim-EL protein after BCR stimulation (Fig. 5*A*). These results suggest reciprocal Mcl-1 and Bim expression is dictated by the PI3K pathway. We thus monitored the phosphorylation of Akt, a downstream molecule of PI3K, during BCR stimulation. Akt phosphorylation was sustained for longer periods in naive B cells than IgM^+ memory B cells (Fig. 5, *B* and *C*). A previous study showed that PI3K activation is critical for BCR-mediated induction of CD86 and CD69 surface expression in murine B cells (19). As shown in Fig. 1*C*, expression levels of CD86 and CD69 are higher in naive than IgM^+ memory B cells at a late time point. Collectively, these results suggest that reciprocal expression of Mcl-1 and Bim protein in both subsets could be explained by their distinct regulation of the PI3K pathway.

Tcl1 and Gal-1 are the critical mediators for B cell to express Mcl-1 and Bim proteins, respectively

To identify the molecule responsible for sustained activation of the PI3K pathway, we conducted gene expression profiling of B cell subsets before and after BCR stimulation. A subset of genes displayed >2-fold differences between naive and IgM^+ memory B cells (data not shown). Among these genes, we focused on Tcl1, a potent Akt kinase coactivator (20, 21). We tested Tcl1 mRNA expression in both subsets (Fig. 6*A*). In the absence of stimuli, a higher level of Tcl1 mRNA was observed in naive B cells than in IgM^+ memory B cells. BCR stimulation resulted in more than 10-fold mRNA induction of Tcl1 in naive B cells. We next evaluated the level of Tcl1 protein in both subsets (Fig. 6*B*). Tcl1 protein was detected only in naive B cells irrespective of stimulation. Reduction in the expression of Tcl1 protein implies the existence of a posttranscriptional inhibitory mechanism of Tcl1 expression. To determine whether Tcl1 expression can induce Mcl-1 expression to promote B cell survival, Tcl1 transgene was overexpressed in IgM^+ memory B cells. Enforced Tcl1 expression induced a high level of Mcl-1 expression in IgM^+ memory B cells and protected their apoptotic cell death (Fig. 6, *C* and *D*). Thus, Tcl1 expression in naive, but not IgM^+ memory B cells plays a critical role in Mcl-1 expression that in turn promotes their survival.

We also sought to identify a molecule involved in Bim expression and apoptosis in IgM^+ memory B cells. In a list of genes identified in microarray analysis, higher levels of a glycoprotein Gal-1 in IgM^+ memory B cells were noted (data not shown). In the absence of stimuli, Gal-1 mRNA was more expressed in IgM^+ memory B cells and BCR stimulation of this subset caused drastic mRNA induction of this gene (Fig. 7*A*). Consistent with its mRNA expression, Gal-1 protein was abundantly expressed in IgM^+ memory B cells (Fig. 7*B*). To test whether Gal-1 expression can induce Bim expression in B cells and enhance their apoptosis, *Gal-1* transgene was overexpressed in naive B cells. Enforced *Gal-1* expression resulted in higher levels of Bim expression in naive B cells, which is associated with the increment of apoptotic cells by >2-fold (Fig. 7, *C* and *D*). These results suggest that Gal-1 plays a vital role in promoting Bim expression and inducing apoptosis in IgM^+ memory B cells. Interestingly, Gal-1 also functions

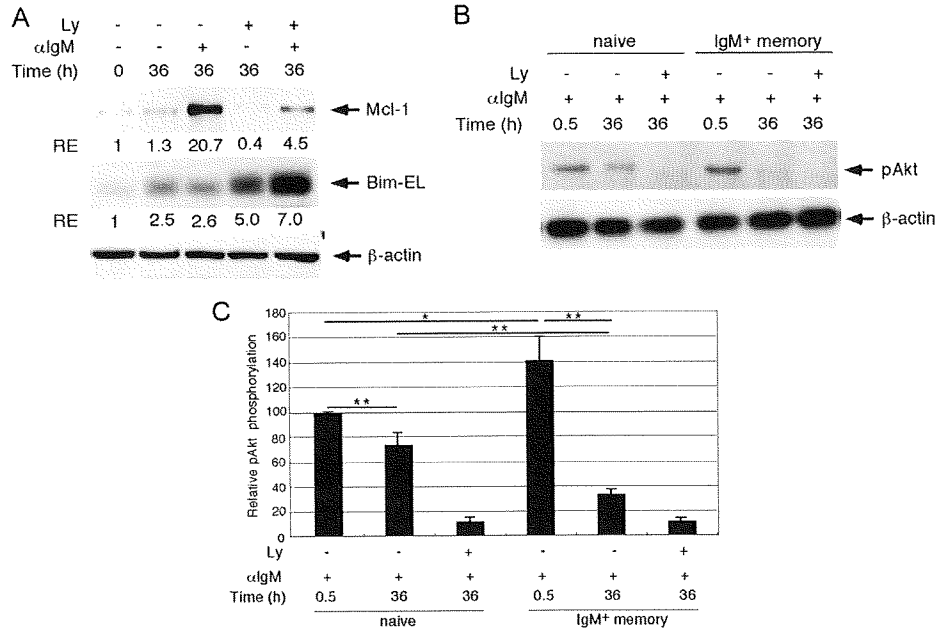

FIGURE 5. Regulation of Mcl-1 and Bim protein expression by the PI3K pathway. *A*, Naive B cells were pretreated with or without Ly294002 (Ly; 10 μM) for 30 min and stimulated for 36 h in the absence or presence of 20 μg/ml F(ab')$_2$ goat anti (α)-hIgM. Cell lysates were separated on a 12.5% SDS-PAGE gel, and analyzed by western blotting with anti-Bim, -Mcl-1 sera, and anti-β-actin mAb. The results shown are representative of three independent experiments. *B*, Naive and IgM$^+$ memory B cells were pretreated with or without Ly294002 (10 μM) for 30 min and stimulated for the indicated time periods in the absence or presence of 20 μg/ml F(ab')$_2$ goat anti-human IgM. Cell lysates were separated on a 10% SDS-PAGE gel and analyzed by Western blotting with anti-phospho-Akt sera and anti-β-actin mAb. Results are representative of three independent experiments. *C*, Densitometric analyses of Akt phosphorylation in B cell subsets. The resulting values were expressed as the percentage in reference to that of BCR-stimulated naive B cells at 0.5 h. Values are the mean SD of three independent experiments. *, $p < 0.05$; **, $p < 0.01$.

as a soluble cytokine (22). Because activation of Akt and JNK is critical for regulating Bim expression (23, 24), we tested the effect of recombinant Gal-1 on BCR-induced phosphorylation of Akt and JNK in B cells. As shown in Fig. 7*E*, Gal-1 remarkably inhibited Akt phosphorylation, whereas it slightly enhanced JNK phosphorylation in B cells upon BCR stimulation. Taken together, Gal-1 regulates Bim expression through its effects on activation of Akt and JNK in B cells.

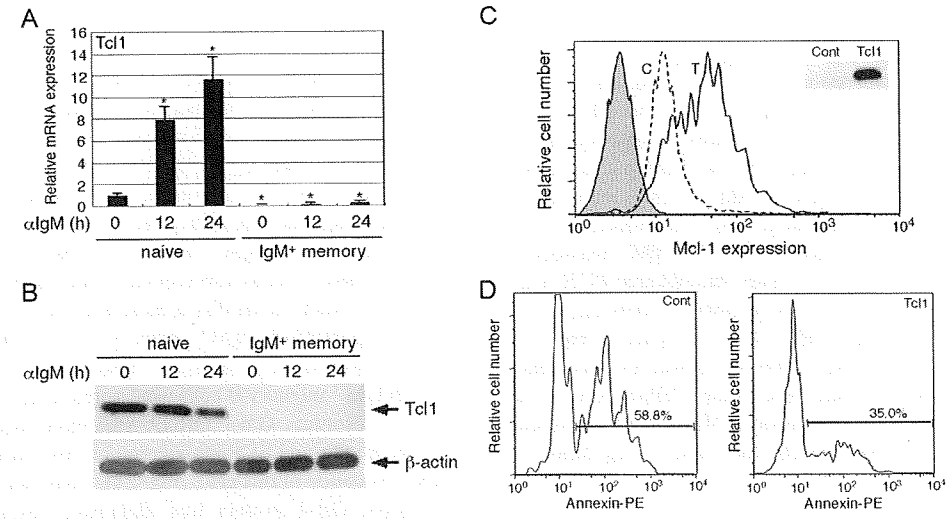

FIGURE 6. Tcl1 is critical for Mcl-1 expression and survival of B cell subsets. Naive and IgM$^+$ memory B cells were incubated for the indicated time intervals in the absence or presence of 20 μg/ml F(ab')$_2$ goat anti (α)-hIgM. *A*, Quantitation of Tcl1 mRNA by real-time PCR in naive and IgM$^+$ memory B cells. Data are normalized to the expression of 18S rRNA. Results are representative of five independent experiments. *, $p < 0.01$ (with reference to unstimulated naive B cells). *B*, Cell lysates were separated on a 12.5% SDS-PAGE gel, and analyzed by Western blotting with anti-Tcl1 sera, and anti-β-actin mAb. Results are representative of four independent experiments. IgM$^+$ memory B cells were transfected with either pEGFP-empty or -Tcl1 for 18 h and then stimulated with 20 μg/ml F(ab')$_2$ goat anti-hIgM for 24 h. *C*, After culture, intracellular Mcl-1 expression of GFP-positive cells was analyzed by flow cytometry. *Insets*, Expression of Tcl1 transgene. Results are representative of three independent experiments. *D*, After culture, GFP-positive cells were stained with PE-labeled annexin V and analyzed using flow cytometry. Percentages of annexin-positive cells are shown. Results are representative histogram of three independent experiments. Cont, Control.

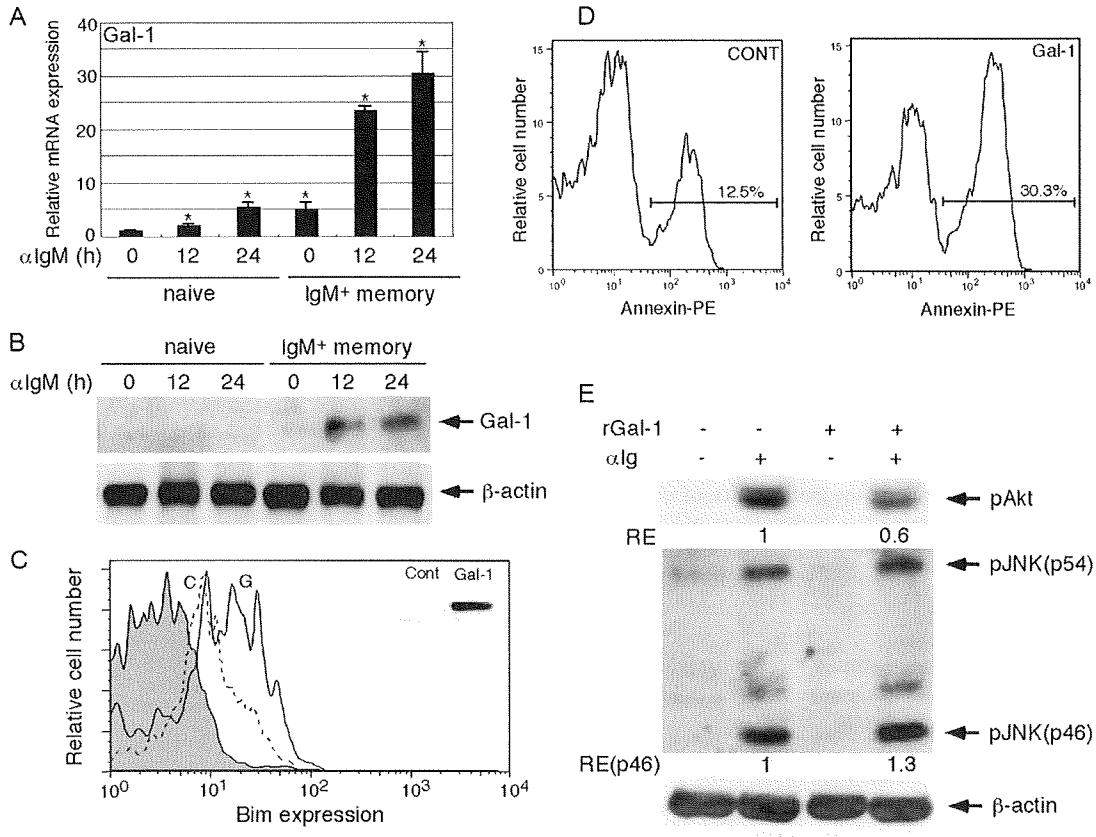

FIGURE 7. Gal-1 is critical for Bim expression and apoptosis of B cell subsets. Naive and IgM^+ memory B cells were incubated for the indicated time intervals in the absence or presence of 20 μg/ml $F(ab')_2$ goat anti (α)-hIgM. *A*, Quantitation of Gal-1 mRNA by real-time PCR in naive and IgM^+ memory B cells. Data are normalized to the expression of 18S rRNA. The results shown are representative of four independent experiments; *, $p < 0.01$ (with reference to unstimulated naive B cells). *B*, Cell lysates were separated on a 12.5% SDS-PAGE gel, and analyzed by Western blotting with anti-Gal-1 sera, and anti-β-actin mAb. Results are representative of three independent experiments. Naive B cells were transfected with either pEGFP-empty or -Gal-1 for 18 h and then stimulated with 20 μg/ml $F(ab')_2$ goat anti-human IgM for 24 h. *C*, After culture, intracellular Bim expression of GFP-positive cells was analyzed by flow cytometry. The insets depict the expression of *Gal-1* transgene. Results are representative of three independent experiments. Cont, Control. *D*, After culture, GFP-positive cells were stained with PE-labeled annexin V and analyzed using flow cytometry. Percentages of annexin-positive cells are shown. Results are representative histograms of three independent experiments. *E*, Human B cells ($CD19^+$) were pretreated with or without recombinant Gal-1 (10 μg/ml) for 12 h and stimulated for 5 min in the absence or presence of 20 μg/ml $F(ab')_2$ goat anti-human IgG/IgA/IgM. Cell lysates were separated on a 10% SDS-PAGE gel, and analyzed by Western blotting with anti-phospho-Akt, -JNK sera, and anti-β-actin mAb. The results shown are representative of three independent experiments. RE, Relative expression.

Discussion

Our study shows that BCR stimulation rescued naive B cells from apoptosis with Mcl-1 induction, whereas it rather accelerated apoptosis of IgM^+ memory B cells with Bim induction. Sustained Akt activation in naive but not IgM^+ memory B cells appears to be critical for reciprocal expression pattern of these Bcl-2 family proteins. Tcl1 and Gal-1, abundantly expressed in naive and IgM^+ memory B cells, respectively, play a crucial role in regulating Akt activation, thereby affecting their survival and death via the Bcl-2-regulated pathway.

BCR signals regulated Mcl-1 expression primarily at the protein level (Fig. 4*B*), presumably because Akt up-regulates Mcl-1 post-transcriptionally via regulating activation of glycogen synthase kinase-3 (25). Sustained Akt activation in naive B cells (Fig. 5, *B* and *C*) may thus be indispensable for continuous replenishment of Mcl-1 protein due to extraordinary short half-life of Mcl-1 (26). In contrast to Mcl-1, Bim transcription is negatively regulated by Akt through via regulating activation of the forkhead transcription factor FOXO3a (27). A small but significant increase in Bim mRNA in IgM^+ memory B cells (Fig. 4*A*) in response to BCR stimulation might be induced by immediate inactivation of Akt (Fig. 5, *B* and *C*) in this subset. Thus, Akt signals might play a critical role in controlling Mcl-1 and Bim expression reciprocally in these B cell subsets.

In contrast to BCR-induced death, spontaneous cell death is more pronounced in naive than in IgM^+ memory B cells (Fig. 3*A*). In addition, 2-day culture of naive B cells without stimuli caused a further decrease in mitochondrial membrane potential (Fig. 3*C*), suggesting that spontaneous cell death is regulated at the mitochondrial level presumably by Bcl-2 family proteins. We, however, found that in the absence of stimuli, expression levels of Bim and Mcl-1 in naive and IgM^+ memory B cells are comparable (data not shown). Therefore, Bim-Mcl-1 balances are not the main determinant of spontaneous cell death in two subsets. Collectively, Bim-Mcl-1 balances can regulate activation-induced death of B cell subsets, whereas other Bcl-2 family proteins might be more critical for the longevity of B cell subsets in the periphery.

We show here that Tcl1 and Gal-1 are differentially expressed in human naive and IgM^+ memory B cells. Tcl1 interacts with Akt and functions as a potent Akt coactivator (20, 21). In Tcl1-deficient mice, the number of splenic follicular, germinal center, and MZ B cells is reduced (28). Our data suggest that Tcl1 positively

regulates Akt activation, resulting in Mcl-1 expression in B cells (Fig. 6). To date, three Tcl1 isoforms have been identified in mice and humans: Tcl1, TCL1B, and MTCP1. Our analysis showed that Tcl1 and MTCP1 but not TCL1B mRNA are expressed in human naive and IgM^+ memory B cells, whereas the expression level of Tcl1 mRNA is different between the subsets (data not shown). These data suggest that the difference in Tcl1 expression between the subsets (Fig. 6) does not reflect the expression patterns of Tcl1 isoforms in each subset. In contrast to Tcl1, Gal-1 induced Bim protein and enhances apoptosis in B cells (Fig. 7, *C* and *D*). Furthermore, Gal-1 significantly inhibited BCR-dependent activation of Akt, leading to the up-regulation of proapoptotic Bim (Fig. 7, *C* and *E*). Gal-1 slightly enhanced BCR-induced JNK phosphorylation (Fig. 7*E*). Because JNK activation positively regulates Bim-induced apoptosis (24, 29), Gal-1 may induce Bim expression in IgM^+ memory B cells also by positively regulating JNK activation.

Gal-1 may play a critical role in the maintenance of B cell tolerance. In fact, anergic B cells express higher levels of Gal-1 than wild-type cells do (30). Gal-1 induces tolerogenic dendritic cells and promotes the expansion of regulatory T cells in vivo (31). In addition, a high level of Gal-1 is required for naturally occurring $CD4^+CD25^+$ T cells to maintain their optimal T_{reg} function (32). These data raise an interesting possibility that human IgM^+ memory B cells play a critical role in the regulation of DC and Treg functions through Gal-1 production. In contrast, abnormal expression of Tcl1 could link to the pathogenesis of B cell malignancies. Tcl1-transgenic mice reveal an expansion of the $CD5^+IgM^+$ population that is reminiscent of human B cell chronic lymphocytic leukemia (CLL) (33), and high Tcl1 expression in human B cell CLL correlates with an aggressive CLL phenotype showing unmutated Ig variable region genes and ZAP70 positivity (34). These data collectively suggest that fine-tuning of the balance between Gal-1 and Tcl1 expression is critical for the homeostasis of human B cell subsets.

Random generation of BCRs results in the emergence of a large number of self-reactive B cells, together with pathogen-specific B cells. BCR-induced cell death and anergy are thus critical for purging or silencing self-reactive B cells. However, there are significant differences in self-reactivity between human B cell subsets: in healthy individuals; up to 20% of mature naive B cells express self-reactive BCRs, whereas IgM^+ memory B cells are devoid of such self-reactive BCRs (5, 6). Bim plays a critical role in BCR-induced cell death and anergy based on the fact that Bim deficiency causes a substantial expansion of autoreactive B cells leading to autoimmune diseases (10, 35). Thus, Bim expression in IgM^+ memory B cells may serve a novel safeguard mechanism that allows efficient elimination or inactivation of the self-reactive repertoire. Our data suggest that the balance between Mcl-1 and Bim is critical in determining B cell survival and death. It has been shown that constitutive expression of B cell-activating factor of the TNF family (BAFF), a survival-promoting cytokine for murine B cells, can break B cell tolerance through expanding self-reactive B cell populations in MZ (36, 37). BAFF exerts its effects on murine B cell survival through down-regulating Bim and up-regulating Mcl-1 (38, 39). We found that BCR-induced death in human IgM^+ memory B cells is abrogated in the presence of BAFF (data not shown). Because patients with systemic lupus erythematosus and Sjögren's syndrome have elevated levels of serum BAFF (37), it is important to test whether self-reactive IgM^+ memory B cells are expanded in these autoimmune diseases.

In summary, BCR signaling dictates survival and death in human naive and IgM^+ memory B cells, respectively. These phenotypes are driven by reciprocal expression of Bcl-2 family proteins such as Mcl-1 and Bim in these B cell subsets. Tcl1 and Gal-1 are expressed in naive and IgM^+ memory B cell subsets, respectively. Tcl1 and Gal-1 might play critical roles in the expression of Mcl-1 and Bim, at least through regulating Akt activation. Therefore, a unique set of molecules such as Tcl1 and Gal-1 defines distinct BCR signaling cascades, dictating fate of human naive and IgM^+ memory B cells.

Disclosures

The authors have no financial conflict of interest.

References

1. Klein, U., K. Rajewsky, and R. Küppers. 1998. Human immunoglobulin $(Ig)M^+IgD^+$ peripheral blood B cells expressing the CD27 cell surface antigen carry somatically mutated variable region genes: CD27 as a general marker for somatically mutated (memory) B cells. *J. Exp. Med.* 188: 1679–1689.
2. Weller, S., M. C. Braun, B. K. Tan, A. Rosenwald, C. Cordier, M. E. Conley, A. Plebani, D. S. Kumararatne, D. Bonnet, O. Tournilhac, G. Tchernia, et al. 2004. Human blood IgM "memory" B cells are circulating splenic marginal zone B cells harboring a prediversified immunoglobulin repertoire. *Blood* 104: 3647–3654.
3. Kruetzmann, S., M. M. Rosado, H. Weber, U. Germing, O. Tournilhac, H. H. Peter, R. Berner, A. Peters, T. Boehm, A. Plebani, I. Quinti, and R. Carsetti. 2003. Human immunoglobulin M memory B cells controlling *Streptococcus pneumoniae* infections are generated in the spleen. *J. Exp. Med.* 197: 939–945.
4. Tangye, S. G., and K. L. Good. 2007. Human IgM^+CD27^+ B cells: memory B cells or "memory" B cells? *J. Immunol.* 179: 13–19.
5. Wardemann, H., S. Yurasov, A. Schaefer, J. W. Young, E. Meffre, and M. C. Nussenzweig. 2003. Predominant autoantibody production by early human B cell precursors. *Science* 301: 1374–1377.
6. Tsuiji, M., S. Yurasov, K. Velinzon, S. Thomas, M. C. Nussenzweig, and H. Wardemann. 2006. A checkpoint for autoreactivity in human IgM^+ memory B cell development. *J. Exp. Med.* 203: 393–400.
7. Pogue, S. L., T. Kurosaki, J. Bolen, and R. Herbst. 2000. B cell antigen receptor-induced activation of Akt promotes B cell survival and is dependent on Syk kinase. *J. Immunol.* 165: 1300–1306.
8. Strasser, A., H. Puthalakath, L. A. O'Reilly, and P. Bouillet. 2008. What do we know about the mechanisms of elimination of autoreactive T and B cells and what challenges remain. *Immunol. Cell Biol.* 86: 57–66.
9. Youle, R. J., and A. Strasser. 2008. The BCL-2 protein family: opposing activities that mediate cell death. *Nat. Rev. Mol. Cell Biol.* 9: 47–59.
10. Enders, A., P. Bouillet, H. Puthalakath, Y. Xu, D. M. Tarlinton, and A. Strasser. 2003. Loss of the pro-apoptotic BH3-only Bcl-2 family member Bim inhibits BCR stimulation-induced apoptosis and deletion of autoreactive B cells. *J. Exp. Med.* 198: 1119–1126.
11. Gomez-Bougie, P., R. Bataille, and M. Amiot. 2005. Endogenous association of Bim BH3-only protein with Mcl-1, $Bcl\text{-}x_L$ and Bcl-2 on mitochondria in human B cells. *Eur. J. Immunol.* 35: 971–976.
12. Opferman, J. T., A. Letai, C. Beard, M. D. Sorcinelli, C. C. Ong, and S. J. Korsmeyer. 2003. Development and maintenance of B and T lymphocytes requires antiapoptotic MCL-1. *Nature* 426: 671–676.
13. Niiro, H., A. Maeda, T. Kurosaki, and E. A. Clark. 2002. The B lymphocyte adaptor molecule of 32 kD (Bam32) regulates B cell antigen receptor signaling and cell survival. *J. Exp. Med.* 195: 143–149.
14. Niiro, H., and E. A. Clark. 2002. Regulation of B-cell fate by antigen-receptor signals. *Nat. Rev. Immunol.* 2: 945–956.
15. Marshall, A. J., H. Niiro, T. J. Yun, and E. A. Clark. 2000. Regulation of B-cell activation and differentiation by the phosphatidylinositol 3-kinase and phospholipase Cγ pathway. *Immunol. Rev.* 176: 30–46.
16. Deming, P. B., and J. C. Rathmell. 2006. Mitochondria, cell death, and B cell tolerance. *Curr. Dir. Autoimmun.* 9: 95–119.
17. U, M., T. Miyashita, Y. Shikama, K. Tadokoro, and M. Yamada. 2001. Molecular cloning and characterization of six novel isoforms of human Bim, a member of the proapoptotic Bcl-2 family. *FEBS Lett.* 509: 135–141.
18. Huang, H. M., C. J. Huang, and J. J. Yen. 2000. Mcl-1 is a common target of stem cell factor and interleukin-5 for apoptosis prevention activity via MEK/MAPK and PI-3K/Akt pathways. *Blood* 96: 1764–1771.
19. Marshall-Clarke, S., L. Tasker, M. P. Heaton, and R. M. Parkhouse. 2003. A differential requirement for phosphoinositide 3-kinase reveals two pathways for inducible upregulation of major histocompatibility complex class II molecules and CD86 expression by murine B lymphocytes. *Immunology* 109: 102–108.
20. Teitell, M. A. 2005. The TCL1 family of oncoproteins: co-activators of transformation. *Nat. Rev. Cancer* 5: 640–648.
21. Noguchi, M., V. Ropars, C. Roumestand, and F. Suizu. 2007. Proto-oncogene TCL1: more than just as a coactivator for Akt. *FASEB J.* 21: 2273–2284.
22. Camby, I., M. Le Mercier, F. Lefranc, and R. Kiss. 2006. Galectin-1: a small protein with major functions. *Glycobiology* 16: 137R–157R.
23. Moller, C., J. Alfredsson, M. Engstrom, H. Wootz, Z. Xiang, J. Lennartsson, J. I. Jonsson, and G. Nilsson. 2005. Stem cell factor promotes mast cell survival via inactivation of FOXO3a-mediated transcriptional induction and MEK-regulated phosphorylation of the proapoptotic protein Bim. *Blood* 106: 1330–1336.

24. Takada, E., K. Hata, and J. Mizuguchi. 2006. Requirement for JNK-dependent upregulation of BimL in anti-IgM-induced apoptosis in murine B lymphoma cell lines WEHI-231 and CH31. *Exp. Cell Res.* 312: 3728–3738.
25. Maurer, U., C. Charvet, A. S. Wagman, E. Dejardin, and D. R. Green. 2006. Glycogen synthase kinase-3 regulates mitochondrial outer membrane permeabilization and apoptosis by destabilization of MCL-1. *Mol. Cell* 21: 749–760.
26. Michels, J., P. W. Johnson, and G. Packham. 2005. Mcl-1. *Int. J. Biochem. Cell Biol.* 37: 267–271.
27. Dijkers, P. F., R. H. Medema, J. W. Lammers, L. Koenderman, and P. J. Coffer. 2000. Expression of the pro-apoptotic Bcl-2 family member Bim is regulated by the forkhead transcription factor FKHR-L1. *Curr. Biol.* 10: 1201–1204.
28. Kang, S. M., M. G. Narducci, C. Lazzeri, A. M. Mongiovi, E. Caprini, A. Bresin, F. Martelli, J. Rothstein, C. M. Croce, M. D. Cooper, and G. Russo. 2005. Impaired T- and B-cell development in Tcl1-deficient mice. *Blood* 105: 1288–1294.
29. Hubner, A., T. Barrett, R. A. Flavell, and R. J. Davis. 2008. Multisite phosphorylation regulates Bim stability and apoptotic activity. *Mol. Cell* 30: 415–425.
30. Clark, A. G., S. Chen, H. Zhang, G. F. Brady, E. K. Ungewitter, J. K. Bradley, F. N. Sackey, and M. H. Foster. 2007. Multifunctional regulators of cell growth are differentially expressed in anergic murine B cells. *Mol. Immunol.* 44: 1274–1285.
31. Blois, S. M., J. M. Ilarregui, M. Tometten, M. Garcia, A. S. Orsal, R. Cordo-Russo, M. A. Toscano, G. A. Bianco, P. Kobelt, B. Handjiski, et al. 2007. A pivotal role for galectin-1 in fetomaternal tolerance. *Nat. Med.* 13: 1450–1457.
32. Garin, M. I., C. C. Chu, D. Golshayan, E. Cernuda-Morollon, R. Wait, and R. I. Lechler. 2007. Galectin-1: a key effector of regulation mediated by $CD4^+CD25^+$ T cells. *Blood* 109: 2058–2065.
33. Bichi, R., S. A. Shinton, E. S. Martin, A. Koval, G. A. Calin, R. Cesari, G. Russo, R. R. Hardy, and C. M. Croce. 2002. Human chronic lymphocytic leukemia modeled in mouse by targeted TCL1 expression. *Proc. Natl. Acad. Sci. USA* 99: 6955–6960.
34. Herling, M., K. A. Patel, J. Khalili, E. Schlette, R. Kobayashi, L. J. Medeiros, and D. Jones. 2006. TCL1 shows a regulated expression pattern in chronic lymphocytic leukemia that correlates with molecular subtypes and proliferative state. *Leukemia* 20: 280–285.
35. Oliver, P. M., T. Vass, J. Kappler, and P. Marrack. 2006. Loss of the proapoptotic protein, Bim, breaks B cell anergy. *J. Exp. Med.* 203: 731–741.
36. Batten, M., J. Groom, T. G. Cachero, F. Qian, P. Schneider, J. Tschopp, J. L. Browning, and F. Mackay. 2000. BAFF mediates survival of peripheral immature B lymphocytes. *J. Exp. Med.* 192: 1453–1466.
37. Mackay, F., P. A. Silveira, and R. Brink. 2007. B cells and the BAFF/APRIL axis: fast-forward on autoimmunity and signaling. *Curr. Opin. Immunol.* 19: 327–336.
38. Craxton, A., K. E. Draves, A. Gruppi, and E. A. Clark. 2005. BAFF regulates B cell survival by downregulating the BH3-only family member Bim via the ERK pathway. *J. Exp. Med.* 202: 1363–1374.
39. Woodland, R. T., C. J. Fox, M. R. Schmidt, P. S. Hammerman, J. T. Opferman, S. J. Korsmeyer, D. M. Hilbert, and C. B. Thompson. 2008. Multiple signaling pathways promote B lymphocyte stimulator dependent B-cell growth and survival. *Blood* 111: 750–760.